



university of  
groningen

faculty of science  
and engineering

---

# Inverted Pendulum Demonstrator

Industrial Engineering and Management  
Bachelor Thesis 2018

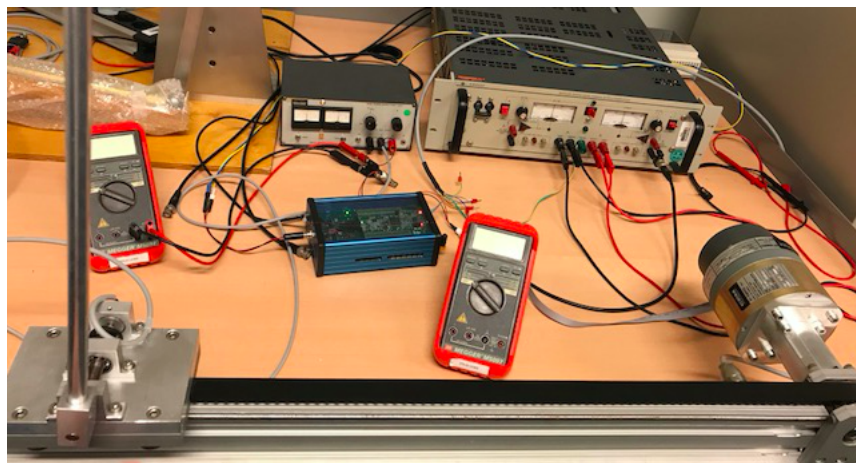
---

Rosalie van Oosterhout

S2857553

r.van.oosterhout@student.rug.nl

Supervisors: ing. M.(Martin) Stokroos and G.K.H.(Gunn) Larsen, dr.



## 1 Abstract

The Inverted Pendulum is the classical textbook control problem of an inherently unstable system. This system is used to demonstrate the target hardware platform for Matlab/Simulink developed by the DTPA group, based on a 32-bit microcontroller. With this platform it is possible to run Simulink models and controllers in real-time while connecting these models with input/output signals from the real world. The Inverted Pendulum demonstrator is not yet working at the University of Groningen. A controller has to be designed to keep the pendulum upwards in its vertical position, the inverted pendulum. First the system is analyzed when the pendulum is in its downwards vertical position, the normal pendulum, to verify the model in the plant with open-loop. Only at the end when testing the controller, the inverted pendulum is evaluated.

The Inverted Pendulum demonstrator is build up of a transport rail, a cart, a DC-motor, a sensor that measures the angle of the pendulum, a sensor that measures the position of the cart, the pendulum, the target-hardware platform and the amplifier that drives the motor. In order to obtain a controller for the system, first the system has to be analysed by the use of mathematical modelling and simulation to obtain the correct models corresponding to the system. The input of the mechanical subsystem is the force and the output is the angle of the pendulum and the position of the cart. Thereafter, the unknown values of the variables of the system are either determined or obtained. Moreover, the motor is analyzed to obtain the torque as a function of the current, from which due to mechanical translation the force can be obtained. Besides this, also the encoder, which reads the position of the cart, and the potentio-meter, which reads the angle of the pendulum, are analyzed and the y-axes corresponding to the outputs translated to meters, meters per second and degrees. Thereafter, different circuits corresponding to the plant and interaction between the computer and the plant (see figure 2) have to be obtained to gain clear understanding of the system. This is because there is an interaction between the plant (figure 2) and the PC. In order to enable communication between the PC and the plant Simulink models with connection blocks between the PC and the plant are obtained in discrete-time.

After having obtained the correct models corresponding to the system, the PID-controller is designed both in Matlab and Simulink. When testing the controller for the normal pendulum, the PID-controller seemed to be correct. Before testing the controller for the inverted pendulum, a switch is added to the model with connection blocks between the PC and the plant in order to limit the transport rail at certain positions to ensure safety. It turned out, that the PID-controller when applying it to the inverted pendulum needed some optimization. Moreover, as already concluded from simulations, the position of the cart, which is dependent on the angle of the pendulum, was not yet controlled. This problem is solved by adding an offset to the angle measurement that is proportional to the position of the cart. Besides this, also a derivative controller corresponding to the position is added as offset to the angle measurement. This way, the cart will go to the center of the transport rail by which the position of the cart is controlled. When testing this, it turned out that the control system is optimal for this pendulum, but resonance in the aluminium pendulum occurred. Because it is difficult to find where in the system the resonance is coming from, a hollow, plastic inverted pendulum is tested on the system to avoid resonance. The resonance was now removed, but the control system was not optimal anymore under the same conditions compared to the the aluminium inverted pendulum. The hollow, plastic pendulum has its mass at the end of the pendulum and has a different length than the aluminium pendulum. Therefore, it cannot be compared to the models obtained for the aluminium pendulum. So, either the resonance has to be removed from the system with the aluminium inverted pendulum, or new models have to be obtained corresponding to the hollow, plastic inverted pendulum in order to obtain the correct PID-controller for this pendulum.

**Contents**

1	Abstract . . . . .	1
2	Introduction . . . . .	5
3	Analysis of research context and problem . . . . .	6
3.1	Problem statement . . . . .	6
3.2	Stakeholder analysis . . . . .	6
4	Scope of research . . . . .	7
4.1	Cycles of Hevner . . . . .	7
4.2	Scope . . . . .	7
5	System description . . . . .	7
5.1	Current situation . . . . .	7
5.2	Inverted Pendulum control system . . . . .	8
5.3	Transport rail . . . . .	9
5.4	DC servo-motor . . . . .	10
5.5	Cart position sensor . . . . .	10
5.6	Pendulum angle sensor . . . . .	10
5.7	The power amplifier . . . . .	11
5.8	Target-hardware platform and PC . . . . .	11
5.9	PID-controller . . . . .	11
5.10	Model-based controller . . . . .	12
6	Goal of research . . . . .	12
7	Research questions . . . . .	12
8	Research methods . . . . .	13
8.1	Modelling . . . . .	13
8.2	Simulating . . . . .	13
8.3	Experimenting . . . . .	13
8.4	Literature Research . . . . .	14
9	Risk analysis and feasibility . . . . .	14
10	Project overview . . . . .	14
11	Mathematical modelling . . . . .	15
11.1	Equations of motion . . . . .	16
11.1.1	Vertical position of the pendulum . . . . .	16
11.1.2	Horizontal position of the pendulum . . . . .	17
11.2	Langrange equation . . . . .	18

11.2.1	Kinetic energy . . . . .	18
11.2.2	Potential energy . . . . .	18
11.2.3	Total Langrange equation . . . . .	18
11.3	Euler-Langrange equations . . . . .	19
11.4	Linearization . . . . .	19
11.5	Laplace transform . . . . .	20
11.6	Transfer functions . . . . .	20
11.6.1	Transfer function of the angle of the pendulum . . . . .	20
11.6.2	Transfer function of the cart . . . . .	20
11.7	State-space . . . . .	21
12	Simulating . . . . .	22
12.1	Simulink model 1 . . . . .	22
12.2	Transfer functions . . . . .	24
12.3	State-space . . . . .	25
13	Calculating unknown variables . . . . .	26
13.0.1	The length of the pendulum (l) . . . . .	26
13.0.2	Mass of the pendulum (m) . . . . .	26
13.0.3	Mass of the cart (M) . . . . .	26
13.0.4	Mass moment of inertia of the pendulum (I) . . . . .	27
13.0.5	Coefficient of friction (b) . . . . .	27
14	Model validation . . . . .	28
15	Potentio-meter . . . . .	29
16	The encoder . . . . .	30
17	Scaling of the sensor values . . . . .	31
17.1	Angle of the pendulum . . . . .	32
17.2	Position and speed of the cart . . . . .	32
18	DC-motor . . . . .	33
19	PID-controller . . . . .	36
19.1	The angle of the pendulum . . . . .	36
19.2	The position of the cart . . . . .	37
20	PID in Simulink . . . . .	38
21	Testing Inverted Pendulum . . . . .	39
22	Conclusion . . . . .	41
23	Discussion . . . . .	43
24	Appendix . . . . .	45
25	Bibliography . . . . .	76

## 2 Introduction

This report is about the Inverted Pendulum demonstrator. To explain it in a most basic manner, this is balancing a rod on one finger, only in this case this is done by a computer.

A more complex explanation is that the Inverted Pendulum is a classical textbook-control problem of an inherently unstable system. The idea is that the pendulum, which is fixed on the cart with a pivot, stays upwards in a vertical position, while the cart moves. The Inverted Pendulum demonstrator is already available at other institutions but not yet at the University of Groningen. This Inverted Pendulum demonstrator will be used at the University of Groningen for promotion and as education for the study Industrial Engineering and Management.

The Discrete Technology and Product Automation (DTPA) group already developed the target hardware platform for Matlab/Simulink, which will be used to demonstrate the Inverted Pendulum. The main mission of this research group is to provide a leading education and research environment for students and researchers who are interested in an interdisciplinary study in Engineering, Management, Mathematics, Computer Sciences and Engineering Sciences in general [1]. The idea is that the Inverted Pendulum set-up can be demonstrated with the target hardware platform for Matlab/Simulink developed in the DTPA group. Moreover, it can be used as an illustrative example in education for use in different courses, such as Mechatronic and Control Engineering, but also for information days to promote the study Industrial Engineering and Management. Besides this, in the future, the set-up of the Inverted Pendulum can also be used by Bachelor or Master students to develop advanced control algorithms.

In order to ensure that the Inverted Pendulum demonstrator can be used, there should be a PID controller and a model-based controller for the Inverted Pendulum designed in order to ensure a stable system by keeping the Pendulum upwards in a vertical position. Therefore, there should be a stable Inverted Pendulum set-up developed, which can be demonstrated with the target hardware platform for Matlab/Simulink.

The question that needs to be answered then turns into: How should a working PID and model-based controller be designed to keep the pendulum in a vertical position around the centre position of the horizontal transport rail?

### **3 Analysis of research context and problem**

#### **3.1 Problem statement**

The critical issue is that there should be an Inverted Pendulum set-up developed at the University of Groningen, that can be demonstrated with the target hardware platform for Matlab/Simulink based on 32-bit microcontrollers, that is able to run Simulink models and controllers in real-time while it is possible to connect these models with input/output signals from the real world.

#### **3.2 Stakeholder analysis**

The stakeholder and also the main problem owner is Martin Stokroos, member of support staff of the research group of Discrete Technology and Product Automation (DTPA). The focus of this research group is on developing quantitative and analytic theories and methodologies based on mathematical models for design and control of complex industrial systems and processes [1]. Since the main mission of DTPA is to provide a leading education and research environment for students and researchers, they have a high interest in this. This is because they want to use the Inverted Pendulum demonstrator to educate students about the specific disciplines already mentioned at the University of Groningen. Therefore, this stakeholder can be considered as a key player.

## 4 Scope of research

### 4.1 Cycles of Hevner

The research can be related to two cycles of Hevner (see figure 19 in the appendix). First, it contributes to the rigor cycle because this cycle can be used as a knowledge base in order to for example find the right sensors used. On the other hand, it also contributes to the design cycle. This is because a classic PID-controller and a model-based controller for the Inverted Pendulum have to be designed. Since the deliverable is defined as designing a PID-controller and a model-based controller for the Inverted Pendulum, it relates more to the design cycle.

### 4.2 Scope

The scope of the research is restricted to the Inverted Pendulum demonstrator and the hardware platform of the DTPA group at the University of Groningen. This is because this is the only stakeholder and problem owner. Moreover, the automatically swing-up of the pendulum is ignored due to its complexity. This means that the pendulum will start in a vertical upward position. Actually, first the pendulum in its vertical downwards position is analyzed throughout the project. This is because this makes it easier to analyze the behavior of the pendulum. Another boundary condition is that it only includes the inter-disciplinary studies in Engineering, Management, Mathematics, Computer Science and Engineering Science in general as defined by the research group of DTPA. By clearly stating this specific scope, the research will be achievable and manageable.

## 5 System description

### 5.1 Current situation

The DTPA research group developed a hardware platform for Matlab/Simulink, based on 32-bit microcontrollers, that is able to run Simulink models and controllers in real-time while it is possible to connect these models with input/output signals from the real world. With this hardware platform, the Inverted Pendulum could be demonstrated. The current Inverted Pendulum set-up consists of a transport rail (number 1 in figure 1), a cart (number 2 in figure 1), a sensor for measuring the angle of the pendulum (number 3

in figure 1), a DC-motor (number 4 in figure 1), a sensor to measure the position of the cart (number 5 in figure 1), the inverted pendulum itself (number 6 in figure 1), the amplifier that drives the motor (number 7 in figure 1), the target-hardware platform (number 8 in figure 1) and the PC.

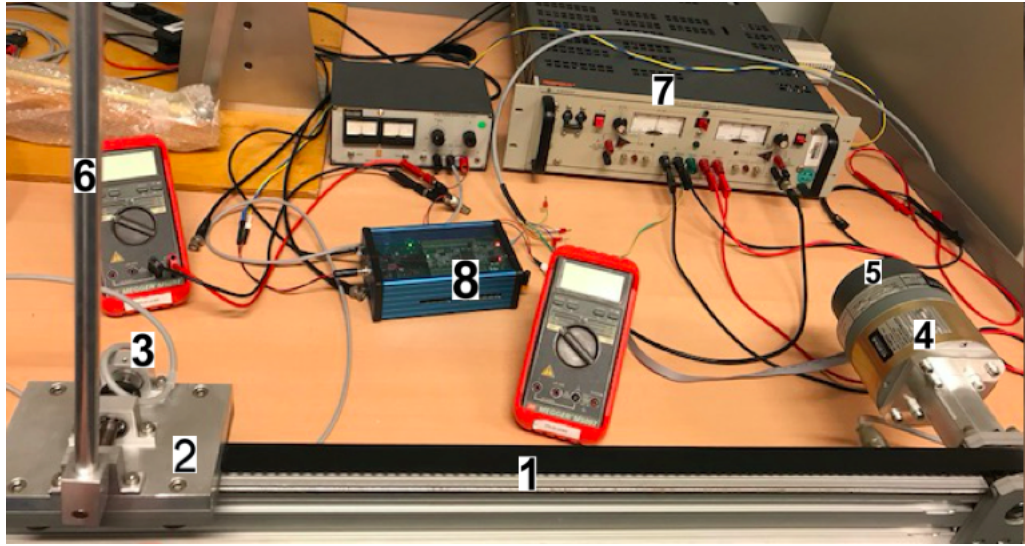


Fig. 1: Set-up of the Inverted Pendulum demonstrator of DTPA lab

## 5.2 Inverted Pendulum control system

The Inverted Pendulum is the classical textbook control problem of a non-linear and unstable dynamic system [2]. The basic schematic of the system is shown in figure 2. The set-up consists of the transport rail, the cart, the servo-motor, the encoder, which is attached to the servo-motor, the pendulum, which is assembled to the cart and the potentio-meter, which is attached to the cart. In order to drive the cart to balance the pendulum, a control algorithm should be used. Therefore, the deviation of the pendulum from its upright position and the position of the cart are significant measurements. The encoder is used to measure the position and speed of the cart. Another sensor used, is the potentio-meter, which measures the angle that the pendulum makes.

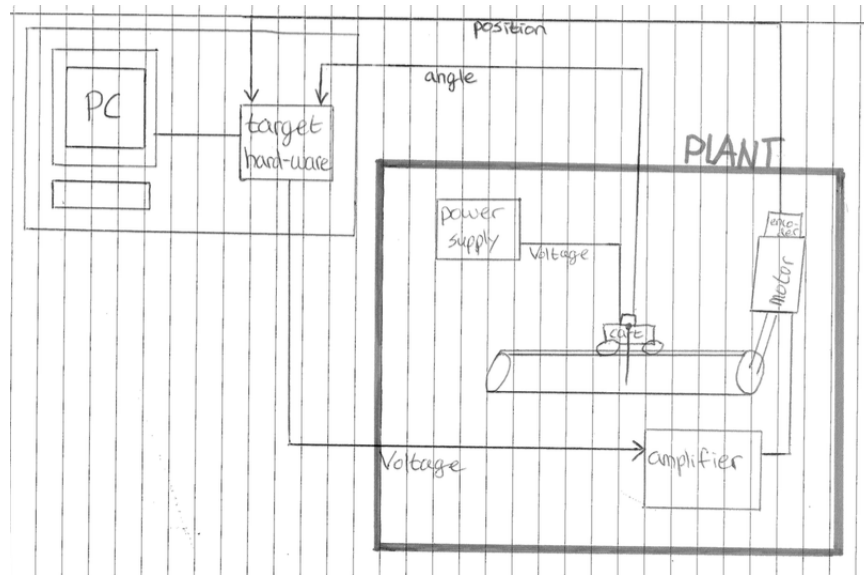


Fig. 2: sketch of the system

### 5.3 Transport rail

In figure 3 a schematic overview of the transport rail is given. The rail consists of a tooth belt, guide, cart and carrier profile. The cart is assembled to the tooth belt. The model corresponding to this transport rail is the ECO 30/60, with the number 02251/1/02. The diameter of the conveyor pulley is 6.621 centimeters (figure 20 of the Appendix)[3].

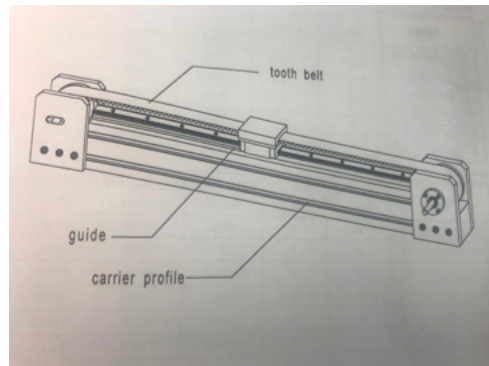


Fig. 3: sketch of transport rail[3]

## 5.4 DC servo-motor

The servo-motor generates the power that is required to move the transport rail. The servo-motor used with its specifications is shown in figure 4. Both the stator and the rotor of the servo-motor contain magnetic coils.

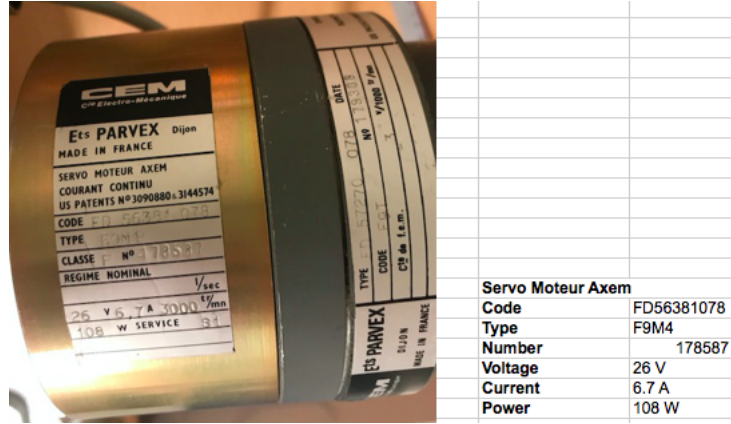


Fig. 4: servo-motor

## 5.5 Cart position sensor

To measure the position of the cart, the encoder is used to measure the position and speed of the cart. Moreover, it provides robust measurements data but requires mechanical coupling to the pendulum and electrical connections to the controller. It translates the rotary motion of the shaft into two-channel digital output. The encoder used is low cost, high performance, two-channel optical increment and emphasizes high reliability and high resolution [4].

## 5.6 Pendulum angle sensor

To measure the angle that the pendulum makes, the potentiometer is used. It is a manually adjustable variable resistor with three terminals of which two terminals are connected to both ends of a resisting element. The third terminal connects to a sliding contact, which breaks the resistance in two halves and moves based on the pendulum swings. [5].

## 5.7 The power amplifier

The power amplifier has the function to drive the motor. It can both work as a Voltage controlled Voltage source or as a Voltage controlled current source. Moreover, a positive inputs generates a negative output and a negative input gives a positive output. The scale of this amplifier is 1:3.6 Voltage.

## 5.8 Target-hardware platform and PC

The target-hardware platform enables running Simulink models and controllers in real-time while connecting these models with the input/output signals of the inverted pendulum demonstrator. The input signals of the target-hardware platform are the signals coming from the potentio-meter and the encoder, which are communicated to the PC. The output of the target-hardware platform is communicated by the PC and defined as the Voltage signal to the amplifier. In order to enable communication between the PC and the real world (the plant), digital-to-analogue (DAC) and analogue-to-digital (ADC) blocks have to be used in Simulink. In specific, the DAC block is used to communicate from the computer to the plant and the ADC blocks are used to communicate the signals from the potentio-meter and the encoder to the PC. This also clarifies the fact that the Simulink models have to be in discrete-time.

## 5.9 PID-controller

One method of designing a control algorithm that uses the rotation of the angle of the pendulum and the positioning of the cart as input measurement is by using the PID-controller. This controller maintains the output of the system to ensure zero error between the desired output and the process variables in closed loop operations [6]. The PID-controller consists of a proportional controller, integral controller and a derivative controller. First, a proportional controller gives output, which is proportional to the current error. The I-controller integrates the error over a period of time until the value of the error becomes zero. Lastly, the derivative controller anticipates future behaviour of the error. In figure 5 a schematic overview of the working of the PID is given.

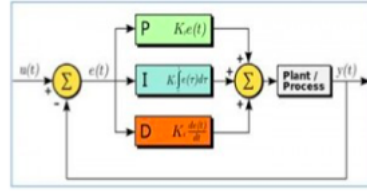


Fig. 5: Overview PID controller[6]

### 5.10 Model-based controller

Using the model-based controller is another method for designing a control algorithm. This method does not use the PID-controller variables but makes use of a closed loop transfer function [7]. A basic schematic overview of a model-based controller is shown in figure 6. After having designed models for these two different methods for the Inverted Pendulum, the methods can be compared to each other.

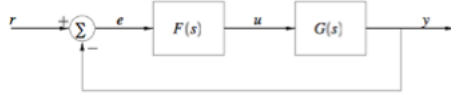


Fig. 6: Schematic overview of model-based controller [7]

## 6 Goal of research

The goal is to develop a stable Inverted Pendulum set-up by designing a classic PID-controller and a model-based controller for the Inverted Pendulum to keep the pendulum in a vertical position around the centre position of the horizontal transport rail, that can be demonstrated by hardware platform designed by the research group of DTPA at the University of Groningen.

## 7 Research questions

How should a working PID and model-based controller be designed to keep the pendulum in a vertical position around the centre position of the horizontal transport rail, that can be demonstrated by the hardware platform designed by the research group of DTPA?

1. What is the influence of the length of the pendulum?
2. What are the equations of motion of the system?
3. What are the equations for the transfer functions and the state-space corresponding to the system?
4. What are the Simulink models corresponding to the system?
5. Which variables can still be determined?
6. How to make sure that Inverted Pendulum stays between certain limits, so that the cart will not bump to the ends of the transport rail.
7. What characteristics of the motor are relevant?
8. What characteristics of the transport rail are relevant?
9. Is the hardware platform designed by DTPA fast enough in computations per second for the Inverted Pendulum?

The sub research questions all contribute to the main research question. In order to obtain the answer to the main research question, all the sub questions have to be answered first.

## **8 Research methods**

Different tools, techniques and methods can be used to answer the sub research questions as defined above. These tools are mainly modelling, simulating, experimenting and some literature research.

### **8.1 Modelling**

Mathematical modelling is a significant tool to obtain the equations of motion, the transfer functions and the state-space equations. Therefore, this tool mostly corresponds to sub questions 2 and 3.

### **8.2 Simulating**

Building models in Simulink is significant in order to validate the designed mathematical models. From these scopes it can be checked if the models are correct. Therefore, this can be considered as a significant tool.

### **8.3 Experimenting**

Experimenting is necessary in order to obtain the model parameters from the plant, which still have to be determined or obtained. Moreover, this tool

is significant in order to measure the performance of the controller.

#### 8.4 Literature Research

This tool should be used to find more information about different parts of the inverted pendulum demonstrator. Moreover, this tool can be used to search more explanation about certain methods used.

### 9 Risk analysis and feasibility

The system has clear boundaries and the steps to be performed according to the sub questioned are defined. Therefore, it should be feasible to answer the main research question. Perhaps, due to time restrictions it might not be possible to create both a PID and a model-based controller. The focus will first be on the PID-controller and thereafter on the model-based controller.

### 10 Project overview

Below in figure 7 an overview of the planning of block 2 is shown. At first, modelling should be done in order to understand the mechanics of the system. Next to modelling, simulations should be done in Matlab/Simulink by the use of the system equations obtained from mathematical modelling. Thereafter, the relevant parameters of the system have to be found by calculations or observations of the system. These parameters can then be used to design the controllers. Lastly, the Inverted Pendulum demonstrator should be tested along with the controllers if the pendulum stays in a vertical upward position.

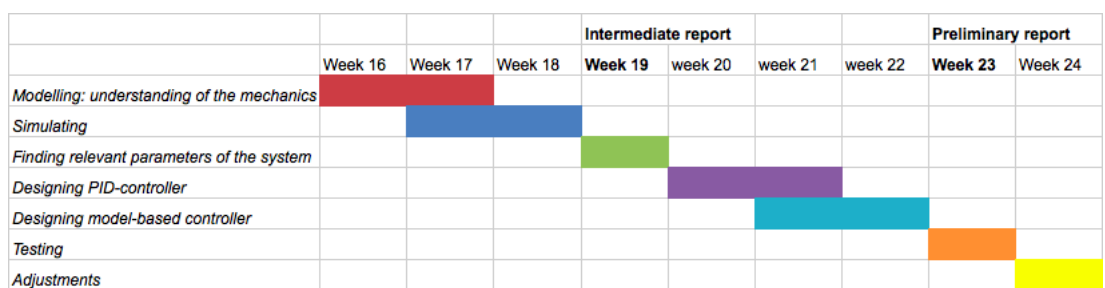


Fig. 7: Planning

## 11 Mathematical modelling

Mathematical modelling is a significant tool to gain a clear understanding of the system. First, throughout the project the pendulum will be analyzed in its vertical downward position, the normal pendulum. This is because this helps validating the parameters of the models for a stable system with similar characteristics. Thereafter, the pendulum when in its vertical upwards position, the inverted pendulum, can be tested by filling in another initial condition ( $\pi$ ) or by adjusting the potentio-meter differently by which the zero point becomes the point when the pendulum is straight in its upwards vertical position.

To understand the dynamics of the system first mathematical modelling has to be applied. In figure 8 a schematic of the cart and the pendulum is given with the applicable forces. Below a list of the relevant variables and its meaning is given:

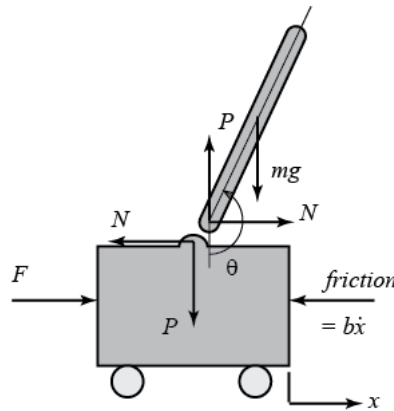


Fig. 8: Schematic of pendulum [10]

$x$  = cart position coordinate

$m$  = mass of the pendulum

$M$  = mass of the cart

$b$  = coefficient of friction of the cart

$I$  = mass moment of inertia of the pendulum

$l$  = length of the pendulum

$F$  = force applied to the mass

$\theta$  = the angle that the pendulum makes

The force is the input of the system, the position of the cart and the angle of the pendulum are the outputs of the system. The variable  $b$  is defined as the coefficient of friction of the cart. Actually, there is also a coefficient of friction for the pendulum, but compared to the friction on the cart the friction on the pendulum is considerably small, which is why the friction of the pendulum is ignored.

## 11.1 Equations of motion

To get an overview of the mechanics of the system, the equations of motion have to be calculated. Moreover, in order to model the pendulum in Simulink, the equations of motion corresponding to figure 8 are significant. Below an overview of the equations is given. Equation 1 belongs to the cart and equation 2 belongs to the angle of the pendulum. In order to calculate the equations for the forces  $P$  and  $N$ , both the vertical and horizontal position of the pendulum have to be taken into account.

$$\ddot{x} = \frac{1}{M}(F - N - b\dot{x}) \quad (1)$$

$$\ddot{\theta} = \frac{1}{I}(-Nl \cos(\theta) - Pl \sin(\theta)) \quad (2)$$

### 11.1.1 Vertical position of the pendulum

$$m\ddot{y}_p = P - mg$$

Then  $P$  becomes:

$$P = m\ddot{y}_p + mg = m(\ddot{y}_p + g) \quad (3)$$

Where:

$$y_p = -l \cos(\theta) \quad (3.1)$$

$$\dot{y}_p = l \sin(\theta) \dot{\theta} \quad (3.2)$$

$$\ddot{y}_p = l \cos(\theta) \dot{\theta}^2 + l \sin(\theta) \ddot{\theta} \quad (3.3)$$

### 11.1.2 Horizontal position of the pendulum

$$x_p = N \quad (4)$$

Where:

$$x_p = x + l \sin(\theta) \quad (4.1)$$

$$\dot{x}_p = \dot{x} + l \cos(\theta) \dot{\theta} \quad (4.2)$$

$$\ddot{x}_p = \ddot{x} + l \cos(\theta) \ddot{\theta} - l \sin(\theta) \dot{\theta}^2 \quad (4.3)$$

N and P then become:

$$N = m(\ddot{x} - l \dot{\theta}^2 \sin(\theta) + l \ddot{\theta} \cos(\theta)) \quad (5)$$

$$P = m(l \dot{\theta}^2 \cos(\theta) + l \ddot{\theta} \sin(\theta) + g) \quad (6)$$

When filling in equations 5 and 6 in equations 1 and 2 the following equations can be obtained:

$$(M+m)\ddot{x} + ml \cos \theta \ddot{\theta} - ml \sin \theta \dot{\theta}^2 = F - b\dot{x} \quad (7)$$

$$(ml^2 + I)\ddot{\theta} + ml \cos \theta \ddot{x} + mgl \sin \theta = 0 \quad (8)$$

The same equations can be obtained by using the method of the Euler-Langrange equations.

## 11.2 Langrange equation

The Langrange equation is another significant mathematical function to obtain the equations of motion. These equations can be used to determine the transfer functions and state-space equations. The general formula of the Langrange equation is composed of kinetic energy and potential energy:

$$L = K - V \quad (9)$$

### 11.2.1 Kinetic energy

The general formula to determine the kinetic energy is:

$$K = \frac{1}{2}Mv_m^2 + \frac{1}{2}mv_m^2 + \frac{1}{2}Iw^2 \quad (10)$$

$$w = \dot{\theta} \quad (11)$$

$$v_m = \dot{x} \quad (12)$$

When applying the general formula to the system (figure 8), the formula corresponding to K becomes:

$$\begin{aligned} K &= \frac{1}{2}M\dot{x}^2 + \frac{1}{2}m\left(\frac{d}{dt}(x + l \sin(\theta))\right)^2 + \frac{1}{2}m\left(\frac{d}{dt}(-l \cos(\theta))\right)^2 + \frac{1}{2}I\dot{\theta}^2 \\ &= \frac{1}{2}M\dot{x}^2 + \frac{1}{2}m((\dot{x} + l \cos(\theta)\dot{\theta})^2 + (l \sin(\theta)\dot{\theta})^2) + \frac{1}{2}I\dot{\theta}^2 \\ &= \frac{1}{2}M\dot{x}^2 + \frac{1}{2}m(\dot{x}^2 + 2l \cos(\theta)\dot{x}\dot{\theta} + l^2 \cos^2(\theta)\dot{\theta}^2 + l^2 \sin^2(\theta)\dot{\theta}^2) + \frac{1}{2}I\dot{\theta}^2 \end{aligned}$$

$$K = \frac{1}{2}(M+m)\dot{x}^2 + \frac{1}{2}ml^2\dot{\theta}^2 + ml \cos(\theta)\dot{x}\dot{\theta} + \frac{1}{2}I\dot{\theta}^2 \quad (13)$$

### 11.2.2 Potential energy

The general formula for potential energy is expressed by equation 14. The potential energy corresponding to the system is expressed by equation 15.

$$V = mgh \quad (14)$$

$$V = -mgl \cos(\theta) \quad (15)$$

### 11.2.3 Total Langrange equation

When filling in equation 9 with equations 13 and 15, the below equation (16) for the total Langrange is obtained.

$$\begin{aligned} L &= \frac{1}{2}(M+m)\dot{x}^2 + \frac{1}{2}ml^2\dot{\theta}^2 + ml \cos(\theta)\dot{x}\dot{\theta} + \frac{1}{2}I\dot{\theta}^2 + mgl \cos(\theta) \\ &= \frac{1}{2}(M+m)\dot{x}^2 + \frac{1}{2}(ml^2 + I)\dot{\theta}^2 + ml \cos(\theta)\dot{x}\dot{\theta} + mgl \cos(\theta) \end{aligned} \quad (16)$$

### 11.3 Euler-Langrange equations

With the use of the final Langrange equation, the Euler-Langrange equations can be determined. Equation 17 shows the general formula for the Euler-Langrange. The final Euler-Langrange corresponding to the position of the cart is given in equation 24. The final Euler-Langrange corresponding to the angle is given in equation 25.

$$\frac{d}{dt} \left( \frac{dL}{dq}(q, \dot{q}) \right) - \frac{dL}{dq}(q, \dot{q}) = Bu - \frac{dD}{dq} \quad (17)$$

$$\frac{dL}{dx} = 0 \quad (18)$$

$$\frac{dL}{d\dot{x}} = (M+m)\dot{x} + ml \cos(\theta)\dot{\theta} \quad (19)$$

$$\frac{dL}{d\theta} = -ml \sin(\theta)\dot{x}\dot{\theta} - mgl \sin(\theta) \quad (20)$$

$$\frac{dL}{d\dot{\theta}} = (ml^2+I)\dot{\theta} + ml \cos(\theta)\dot{x} \quad (21)$$

$$\frac{d}{dt} \left( \frac{dL}{d\dot{x}} \right) = (M+m)\ddot{x} + ml \cos(\theta)\ddot{\theta} - ml \sin(\theta)\dot{\theta}^2 \quad (22)$$

$$\frac{d}{dt} \left( \frac{dL}{d\dot{\theta}} \right) = (ml^2+I)\ddot{\theta} + ml \cos(\theta)\ddot{x} - ml \sin(\theta)\dot{\theta}\dot{x} \quad (23)$$

$$(M+m)\ddot{x} + ml \cos(\theta)\ddot{\theta} - ml \sin(\theta)\dot{\theta}^2 = F - bx \quad (24)$$

$$(ml^2+I)\ddot{\theta} + ml \cos(\theta)\ddot{x} + mgl \sin(\theta) = 0 \quad (25)$$

To conclude, equations 24 and 25 are the same as equations 7 and 8, which ensures that the equations of motion are probably correct. After having build the model in Simulink, it can be concluded from the scopes of both the position of the cart and the angle of the pendulum if the model is indeed correct. Moreover, it can be concluded from equations 24 and 25, that the system is not linear yet. Therefore, these equations first have to be linearized.

### 11.4 Linearization

Before a model can be obtained in Simulink and the transfer functions of both the angle of the pendulum and the position of the cart can be determined from equations 24 and 25, these equations first have to be linearized. Since first the normal pendulum is considered, the pendulum starts in its downward vertical position, and presuming that the pendulum swings through small angles, equations 26, 27, 28 and 29 can be obtained. Therefore, equations 16 and 17 have to be linearized around this point.

$$\theta = 0 \quad (26)$$

$$\cos(\theta) \sim 1 \quad (27)$$

$$\sin(\theta) \sim \theta \quad (28)$$

$$\dot{\theta}^2 \sim 0 \quad (29)$$

This results in the equations of motion expressed by equations 30 and 31.

$$(M+m)\ddot{x} + ml\ddot{\theta} = F - b\dot{x} \quad (30)$$

$$(ml^2+I)\ddot{\theta} + ml\ddot{x} + mgl\theta = 0 \quad (31)$$

## 11.5 Laplace transform

The last step before the transfer function can be obtained is taking the Laplace transform of the linearized equations of motion (30 and 31). Then the following equations can be obtained:

$$(M+m)s^2X(s) + mls^2\theta(s) = F(s) - bsX(s) \quad (32)$$

$$(ml^2+I)s^2\theta(s) + mls^2X(s) + mgl\theta(s) = 0 \quad (33)$$

## 11.6 Transfer functions

### 11.6.1 Transfer function of the angle of the pendulum

From equation 33 can be obtained:

$$\begin{aligned} X(s) &= \frac{-(ml^2+I)s^2 - mgl}{mls^2}\theta(s) \\ &= \left(\left(\frac{ml^2+I}{ml}\right) + \left(\frac{g}{s^2}\right)\right)\theta(s) \end{aligned} \quad (34)$$

When substituting equation 34 in equation 32 the final equation is obtained:

$$\begin{aligned} (M+m)\left(\left(\frac{ml^2+I}{ml}\right) + \left(\frac{g}{s^2}\right)\right)\theta(s)s^2 + b\left(\left(\frac{ml^2+I}{ml}\right) + \left(\frac{g}{s^2}\right)\right)\theta(s)s + mls^2\theta(s) \\ = F(s) \end{aligned} \quad (35)$$

The transfer function of the pendulum can be obtained by equation 35 and then becomes:

$$T_{pend} = \frac{\theta(s)}{F(s)} = \frac{-mls}{s^3 + \frac{b(ml^2+I)}{q}s^2 + \frac{(M+m)gml}{q}s + \frac{bmgsl}{q}} \quad (36)$$

### 11.6.2 Transfer function of the cart

From equation 32 can be obtained:

$$\theta(s) = \frac{-bs - (M+m)s^2}{mls^2}X(s) + \frac{1}{mls^2}F(s)$$

Substitute in equation 33:

$$\frac{(ml^2+I)(-bs-(M+m)s^2)+(mls^2)^2+mgl(-bs-(M+m)s^2)}{mls^2} X(s) = \frac{-(1+mgl)}{mls^2} F(s)$$

The transfer function of the cart then turns into:

$$T_{cart} = \frac{X(s)}{F(s)} = \frac{\frac{(ml^2+I)s^2-gml}{q}}{s^4 + \frac{b(ml+I)}{q}s^3 + \frac{(M+m)gml}{q}s^2 + \frac{bmgl}{\gamma}s} \quad (37)$$

Both transfer functions can be expressed in Matlab (figure 25 of the Appendix). Thereafter, they can be modelled in Simulink.

### 11.7 State-space

State-space is another method, compared to the transfer function, to express the input and output behavior of the system. Actually, the state-space representation is able to combine both the position of the cart and the angle of the pendulum in one expression. In order to express both linearized equations of motion (32 and 33) in state-space form, the variables used in these equations should be expressed in other variables. Below the different variables corresponding to the variables is given in matrix form by 38. From equation 38, both equation 39 and 40 can be concluded. Thereafter, the equations of motion corresponding to the variables defined in 38 can be obtained (41 and 42).

$$\begin{pmatrix} x_1 \\ x_2 \\ x_3 \\ x_4 \end{pmatrix} = \begin{pmatrix} x \\ \dot{x} \\ \theta \\ \dot{\theta} \end{pmatrix} \quad \rightarrow \quad \begin{pmatrix} \dot{x}_1 \\ \dot{x}_2 \\ \dot{x}_3 \\ \dot{x}_4 \end{pmatrix} = \begin{pmatrix} \dot{x} \\ \ddot{x} \\ \dot{\theta} \\ \ddot{\theta} \end{pmatrix} \quad (38)$$

$$\dot{x}_1 = x_2 \quad (39)$$

$$\dot{x}_3 = x_4 \quad (40)$$

$$(M+m)\dot{x}_2 + bx_2 + ml\dot{x}_4 = F \quad (41)$$

$$(ml^2 + I)\dot{x}_4 + ml\dot{x}_2 + mglx_3 = 0 \quad (42)$$

From these equations of motion, both  $\dot{x}_2$  and  $\dot{x}_4$  can be determined (equations 43, 44). Thereafter, the complete state space representation can be

obtained (equation 45):

$$\begin{aligned} \dot{x}_2 &= \frac{-b(ml^2+I)}{(M+m)(Ml+I)-(ml)^2}x_2 + \frac{m^2gl^2}{(M+m)(Ml+I)-(ml)^2}x_3 + \frac{(ml^2+I)}{(M+m)(Ml+I)-(ml)^2}F \\ (43) \quad \dot{x}_4 &= \frac{mlb}{(M+m)(Ml+I)-(ml)^2} - \frac{mgl(M+m)}{(M+m)(Ml+I)-(ml)^2} - \frac{ml}{(M+m)(Ml+I)-(ml)^2}F \end{aligned} \quad (44)$$

$$\begin{pmatrix} \dot{x} \\ \ddot{x} \\ \dot{\theta} \\ \ddot{\theta} \end{pmatrix} = \begin{pmatrix} 0 & 1 & 0 & 0 \\ 0 & b_1 & b_2 & 0 \\ 0 & 0 & 0 & 1 \\ 0 & b_3 & b_4 & 0 \end{pmatrix} \begin{pmatrix} x \\ \dot{x} \\ \theta \\ \dot{\theta} \end{pmatrix} + \begin{pmatrix} 0 \\ w_1 \\ 0 \\ w_2 \end{pmatrix} F$$

$$y = \begin{pmatrix} 1 & 0 & 0 & 0 \\ 0 & 0 & 1 & 0 \end{pmatrix} \begin{pmatrix} x \\ \dot{x} \\ \theta \\ \dot{\theta} \end{pmatrix} + \begin{pmatrix} 0 \\ 0 \end{pmatrix} F \quad (45)$$

$$b_1 = \frac{-(ml^2+I)b}{(M+m)(Ml+I)-(ml)^2} \quad (46)$$

$$b_2 = \frac{m^2gl^2}{(M+m)(Ml+I)-(ml)^2} \quad (47)$$

$$b_3 = \frac{mlb}{(M+m)(Ml+I)-(ml)^2} \quad (48)$$

$$b_4 = \frac{-(M+m)mgl}{(M+m)(Ml+I)-(ml)^2} \quad (49)$$

$$w_1 = \frac{I+ml^2}{(M+m)(Ml+I)-(ml)^2} \quad (50)$$

$$w_2 = \frac{-ml}{(M+m)(Ml+I)-(ml)^2} \quad (51)$$

This state-space representation can also be implemented in Matlab, after which it can be modelled in Simulink. In figure 26 of the Appendix an overview of the Matlab script for the state-space is given.

## 12 Simulating

### 12.1 Simulink model 1

The equations obtained should be modelled in Simulink. In figure 9 an overview of the model corresponding to the linearized equations of equations 1, 2, 5 and 6 is given. The four equations are all in relation with each

other. First, the input of the equation of motion  $\ddot{x}$  is the force. To make the model in figure 9 more clear, the inputs corresponding to the four equations of motion are given below:

$$(1) \quad u(1) = F \quad u(2) = N \quad u(3) = \dot{x} \quad (52)$$

$$(2) \quad u(1) = N \quad u(2) = P \quad u(3) = \theta \quad (53)$$

$$(5) \quad u(1) = \ddot{\theta} \quad u(2) = \theta \quad (54)$$

$$(6) \quad u(1) = \ddot{x} \quad u(2) = \ddot{\theta} \quad (55)$$

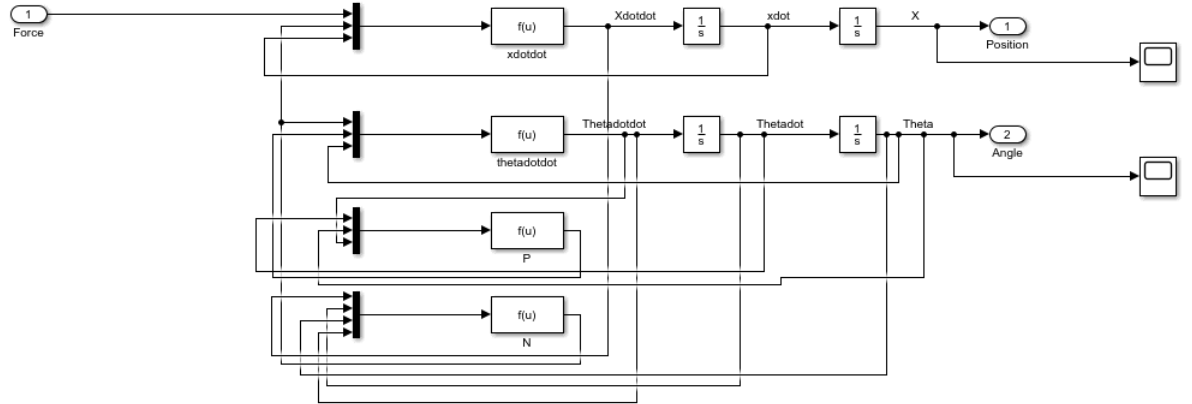


Fig. 9: Simulink model 1

In combination with the different inputs defined above, different formulas correspondent to the  $f(u)$  functions, which are entered into the  $f(u)$  boxes. Below an overview is given:

$$f(u(\ddot{x})) = \frac{1}{M}(u(1) - u(2) - bu(3)) \quad (56)$$

$$f(u(\ddot{\theta})) = \frac{1}{I}(-u(1)l - lu(3)(u(2))) \quad (57)$$

$$f(u_P) = m(l(u(1))u(2) + g) \quad (58)$$

$$f(u_N) = m(u(1) - lu(2)) \quad (59)$$

The input of the system according to figure 8 is the force and the output is the position and the angle. In figure 21 and 22 of the Appendix an overview of the scope of the position of the cart is given when the force is three Newtons, with on the x-axes the time in seconds and on the y-axes the data of the position in pulses.

From these figures of the position of the cart, it can be concluded that the position will go to infinity as the time increases. An explanation for the position of the cart to go to infinity is that the system is still open-loop. This is because there is not yet a controller to make the system closed-loop.

In figure 23 and 24 of the Appendix an overview of the scope of the angle of the pendulum is given. It can be concluded from these figures, that the period  $T$ , in which the pendulum swings back and forth, is around 2.0 seconds, independent of the amplitude of the oscillations. This is in line with the Huygens formula (equation 62) [9], from which  $T$  is 1.9 seconds. For small angles the system can be treated as a simple harmonic oscillator, when moving to higher angles the value for  $T$  will increasingly deviate from the true value. Moreover, it can be concluded that the pendulum oscillates to zero. Besides this, when looking at figure 24, the angle in the beginning is more below zero than at the end, which can be explained by the increasing position of the cart. In the beginning there will be an impulse due to the force on the cart, by which the angle will stay more below zero. To conclude, this model seems to be correct.

$$T = 2\pi\sqrt{\frac{l}{g}} \quad (60)$$

$$l = 0.89 \text{ meter} (\text{assumed}) \quad (61)$$

$$T = 2\pi\sqrt{\frac{0.89}{9.81}} = 1.9 \text{ s} \quad (62)$$

## 12.2 Transfer functions

The transfer function is another expression to model and is obtained from the Laplace transform of the equations of motion. Therefore, the output of these transfer functions should be about the same as the output of Simulink model 1 (figure 9). In figure 10 below an overview of the models of the transfer functions in Simulink is given. It can be concluded, from figures 27, 28, 29, 30 of the Appendix, that this is indeed the case. Therefore, these transfer functions are considered to be correct.

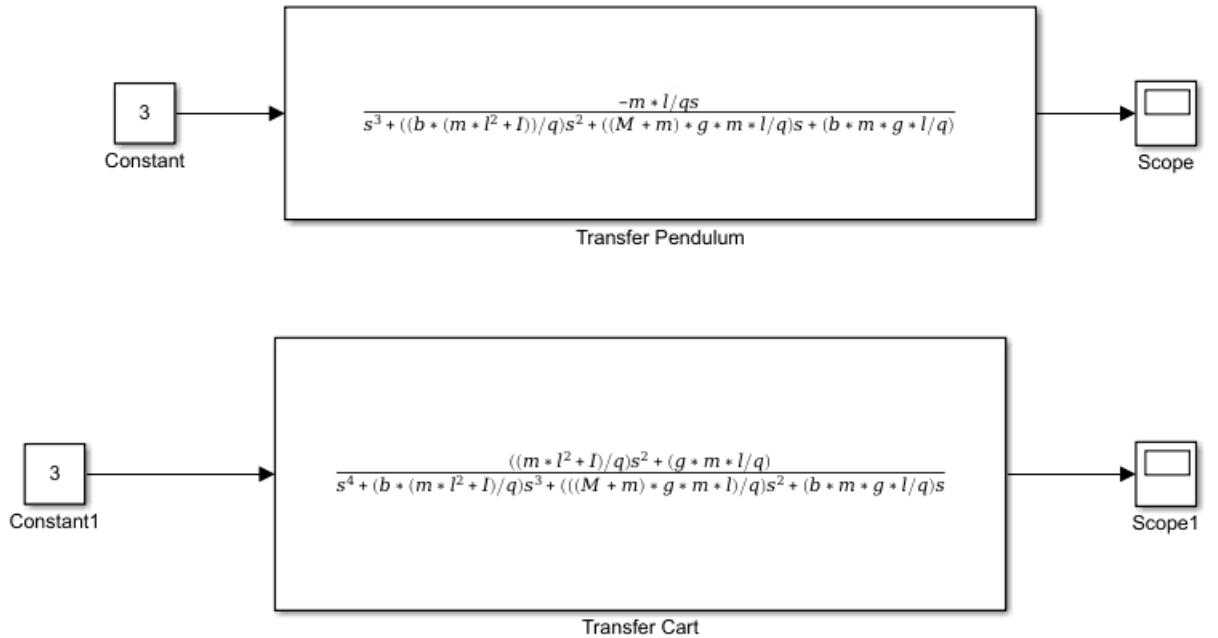


Fig. 10: Simulink model of transfer functions

### 12.3 State-space

The state-space is another method to model the equations of motion. Figure 11 shows the Simulink model designed for the state-space. The output should be the same as both the output of Simulink model 1 and the transfer function. The basic scopes of the state-space are represented by figure 31 and 32 of the Appendix, where the red line corresponds to the angle and the blue line corresponds to the position. In order to obtain a clear overview of the scope of the angle, figures 33 and 34 of the Appendix are obtained to zoom in on the angle only. From these figures it can be obtained, that this is the case. Moreover, the period of Simulink model 1, the transfer function and the state-space is the same (around 2.0 seconds) and corresponds to the result of the equation of Huygens. Therefore, the state-space representation is considered to be correct.

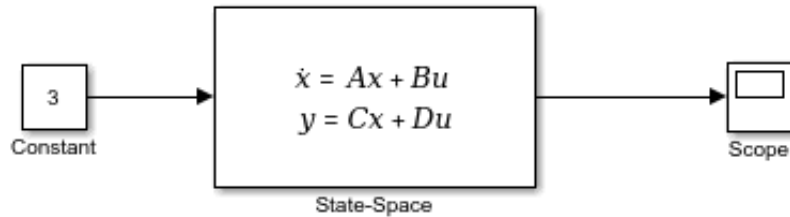


Fig. 11: Simulink model of state-space

## 13 Calculating unknown variables

The unknown variables are the length of the pendulum ( $l$ ), the mass of the pendulum ( $m$ ), the mass of the cart ( $M$ ), the mass moment of inertia ( $I$ ) and the coefficient of friction of the cart ( $b$ ).

### 13.0.1 The length of the pendulum ( $l$ )

The length of the pendulum was chosen to be 0.89 metres. This is because the length should be as long as possible to make the period longer and the system easier to control (as already mentioned previously), but it should not touch the ground.

### 13.0.2 Mass of the pendulum ( $m$ )

The mass of the pendulum is obtained by weighing the pendulum and the following mass is obtained:

$$m = 0.31 \text{ kg} \quad (63)$$

### 13.0.3 Mass of the cart ( $M$ )

The mass of the top size of the cart is weighted and assumed to be 0.6474 kilograms. The mass of the bottom size of the cart and the mass of the wheels should be estimated. The following formulas (64, 65) are used:

$$M = \rho * V \quad (64)$$

$$V = l * w * h \quad (65)$$

With these formulas the following results can be obtained:

$$V_{bottom} = l \cdot w \cdot h = 0.13 \cdot 0.09 \cdot 0.015 = 1.755 \cdot 10^{-4} \text{ m}^3 \quad (66)$$

$$\rho_{aluminium} = 2755 \frac{\text{kg}}{\text{m}^3} [11] \quad (67)$$

$$M_{bottom} = 2755 \cdot 1.755 \cdot 10^{-4} = 0.484 \text{ kg} \quad (68)$$

$$V_{wheels} = \pi \cdot r^2 \cdot h = \pi \cdot (0.027)^2 \cdot 0.017 = 3.89 \cdot 10^{-5} \text{ m}^3 \quad (69)$$

$$\rho_{aluminium} = 2755 \frac{\text{kg}}{\text{m}^3} \quad (70)$$

$$M_{wheels} = 2755 \cdot 3.89 \cdot 10^{-5} = 0.11 \text{ kg} \quad (71)$$

The total mass then turns into:

$$\begin{aligned} M_{total} &= M_{top} + M_{bottom} + M_{wheels} \\ &= 0.6474 + 0.484 + 0.11 = 1.2414 \text{ kg} \end{aligned} \quad (72)$$

#### 13.0.4 Mass moment of inertia of the pendulum (I)

The moment of inertia is measured according to the difficulty of accelerating the pendulum. So with an increasing moment of inertia, it is harder to move the pendulum back and forth and to change its direction, which is why the period increases. The moment of inertia can easily be calculated with the formula for I below (equation 73). Actually, there are two formulas to calculate the moment of inertia. One formula assumes the weight of the system is at the end of the pendulum, while the other formula assumes the systems weight is at the mass center of the pendulum. The latter formula is more accurate, which is why that formula is used (equation 73).

$$I = \frac{ml^2}{3} \quad (73)$$

Since the length of the pendulum is 0.89 metres and the mass of the pendulum is 0.31 kg, the following equation can be obtained:

$$I = \frac{0.31 \cdot (0.89)^2}{3} = 0.082 \frac{\text{kg}}{\text{m}^2} \quad (74)$$

#### 13.0.5 Coefficient of friction (b)

In order to determine the coefficient of friction on the cart, an experiment should be done. In this experiment the angle of the pendulum is not taken into account, just only the position of the cart. When filling in a constant force into the system, the coefficient of friction can be read from the scope of

the speed when the cart slows down. Figure 74 of the Appendix shows the scope of the experiment for 10 seconds. It can be concluded, that around 7 seconds the speed of the cart will go to zero again, of which a zoomed-in version is given in figure 75 of the Appendix. From this figure it can be concluded that the friction coefficient of the cart is around 1 N/m/sec.

## 14 Model validation

To make a final check if the models are indeed correct, the output of the models (Simulink model 1, transfer function and state-space) should be compared to the real system. Therefore, the real system in- and outputs are connected with Simulink through connectors in Simulink (figure 12). In figure 12 a delay block of  $z^{-1}$  is added, from which it can be concluded that this system in Simulink, which communicates to the target-hardware platform, is in discrete-time.

When the pendulum experiences a swing, the scope of the angle result to be the same with the same period T as the outputs of the models. If the pendulum is 90 degrees to the left, from the perspective of standing in front of the demonstrator (-90), the scope of the angle gives a value on the y-axes of -0.5. If the pendulum is 90 degrees to the right (90), the scope of the angle gives a value on the y-axes of 0.5 (figure 59 of the Appendix). These values on the y-axes correspond to the 10 Voltage, which enters the potentio-meter.

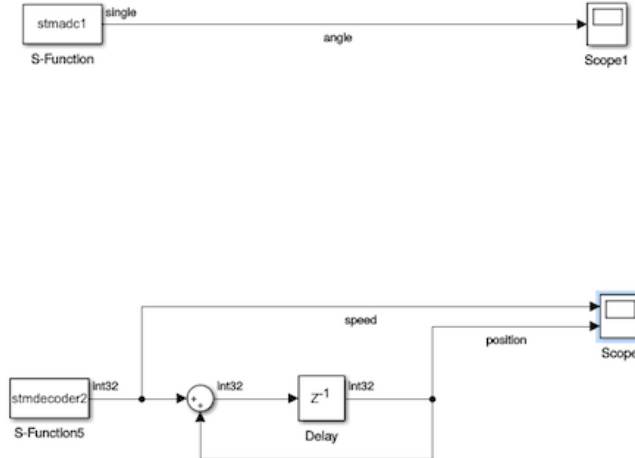


Fig. 12: Simulink model with connection blocks to read the position and the angle

When considering the position and speed of the cart, the scope of the above system shows that the position will go to infinity as well when creating about the same input force as the input force of 3 Newton for the models. Therefore, the models obtained from figure 2 are considered to be correct.

## 15 Potentio-meter

The potentio-meter is used to sense the angular position of the pendulum, which is attached to the rod of the pendulum and connected to one of the ADC blocks from the VHP target 2.0 library in Simulink [5]. The ADC board powers the potentio-meter with 10 Volt and communicates the data to Simulink. The potentio-meter is build up of a slider, that divides the resistance in two halves,  $R_1$  and  $R_2$ , and is attached to a shaft, which is attached to the pendulum. The slider moves based on the pendulum swings. This way it changes the distribution of the total resistance of 10 Volt between  $R_1$  and  $R_2$ , and results to be 5 Volt for each resistor (figure 13 below). This explains the y-axes from -0.5 to 0.5 of the scope of the angle. Figure 43 of the Appendix gives a photo of the potentio-meter used in this project.

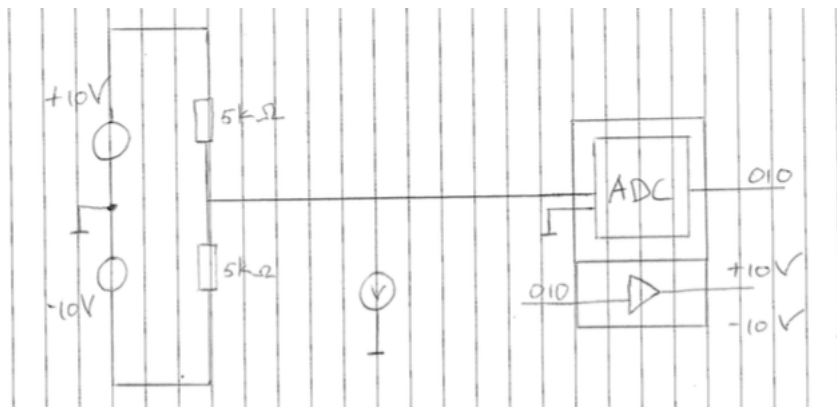


Fig. 13: Circuit potentio-meter and ADC-board

## 16 The encoder

The encoder is attached to the motor and connected to the target hardware platform. Figure 14 below gives an overview of this. The y-axes of the scope of the position and speed of the cart is composed of the number of pulses. This is due to the fact, that the encoder is a sensor used to determine the position and speed of the cart. In general, there are two types of encoders, a rotary and a linear encoder[18]. In this project the rotary encoder, specifically the incremental with quadrature output, is used. These type of encoders have different resolutions, which determine the precision with which the position and speed of the cart can be determined. The resolution is provided by the disk inside the encoder, which has certain number of holes, with a LED on one side of the disk and two photo-sensors on the other side [18]. When light passes through the hole to the photo-sensor, a pulse is send out by the encoder. Figure 41 in the Appendix shows a clear overview of this.

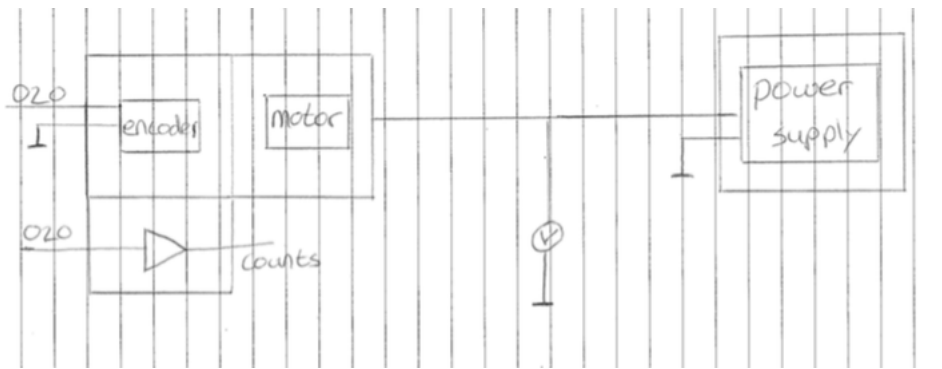


Fig. 14: Circuit encoder and motor

The encoder used in this project is able to make 500 pulses per revolution (PPR) by which the position and speed can be determined. This value can be obtained from the fact, that when one revolution is made the position shows a value on the y-axes of the scope of 2000 pulses. The encoder used is an incremental rotary encoder, which employs two outputs, called quadrature outputs, A and B, because they are 90 degrees out of phase [12]. Figure 37 of the Appendix can be used to decode the direction. When there is a plus one, the cart has moved one half step in the clockwise direction. The notation  $00- > 01- > 11$  means the cart moves forward, and the notation  $00- > 10- > 11$  means the cart moves backwards. From figure 38 of the Appendix it can be concluded that the encoder has a step angle of 90 degrees to make one revolution, and thus has four steps per pulse. Therefore, it can be concluded that the encoder makes 500 PPR, which gives a linear resolution of 2000 PPR ( $4 * 500$ ).

## 17 Scaling of the sensor values

Currently, the the y-axes of the scope of the angle shows the Voltage over the potentio-meter divided by 10. It is more clear to be able to read the angular degrees from the y-axes of this scope. The same holds for the y-axes of the scope of the position and the speed of the cart. Currently, the y-axes of this scope is composed of the number of pulses, given by the encoder. This y-axes of pulses should be turned into meters and meters per second.

### 17.1 Angle of the pendulum

To change the y-axes from Voltage/10 to degrees, measurements have to be done in order to obtain at what value of the y-axes the pendulum is at a certain number of degrees. Below the table is given, which can be obtained from these measurements.

Angular position	-90	-75	-60	-45	-30	-15	0	15	30	45	60	75	90
Voltage/10	-0.5	-0.4	-0.3	-0.2	-0.18	-0.05	0	0.05	0.18	0.2	0.3	0.4	0.5

Then a script in Matlab has to be written denoted by figure 39 of the Appendix. The output of this script is given by figure 40 of the Appendix, where the number of degrees is plotted on the y-axes and the Voltage/10 on the x-axes. It can be concluded, from this figure, that the system is linear and that the fitted data matches the recorded data. In order to obtain the graph, where degrees is on the y-axes and time on the x-axes, the data corresponding to the actual system should be transmitted from Simulink to the workspace in Matlab. This can be done by separate Simulations. In figure 41 an overview of the graph with time on the x-axes and degrees on the y-axes for smaller angles is given. Figure 42 the Appendix gives an overview of the graphs with time on the x-axes and degrees on the y-axes for bigger angles.

### 17.2 Position and speed of the cart

In order to transmit the y-axes of the scope of the position and speed of the cart from pulses, also called counts, to meters and meters per second, calculations can be applied.

The number of pulses should both be translated to meters, by equation 75, and to meters per second, by equation 76. The diameter of the conveyor pulley is 0.06621 meters[3], which is used for these equations. The results of the the calculations for the different counts and counts per sample period as mentioned in the table, are given in the table below:

$$L = \frac{\pi D}{2000} * counts \quad (75)$$

$$Speed = \frac{\pi D}{2000 * T_s} * counts \text{ per sample period} \quad (76)$$

Counts	-6000	-4000	-2000	0	2000	4000	6000
Counts per sample period	-30	-20	-10	0	10	20	30
m	-0.62	-0.42	-0.21	0	0.21	0.42	0.62
m/s	-0.312	-0.208	-0.104	0	0.104	0.208	0.312

In order to plot the meters and meters per second on the y-axes and counts or counts per sample period on the x-axes, a script in Matlab has to be written corresponding to both the position and the speed (figures 43 and 46 of the Appendix). The figures resulting from these scripts are shown in figure 44 and 47 of the Appendix. The minus signs on the y-axes means the cart moves to the left (counterclockwise revolution), when standing in front of the demonstrator. It can be concluded from these figures, that the recorded data matches the fitted data, which means the results can be considered as correct.

To obtain the final curve, where time in seconds is on the y-axes and position in meters or speed in meters per second on the x-axes, the data from the scope of the position and speed of the cart has to be transmitted from Simulink to the workspace in Matlab. This data then can be used to obtain the graphs with meters and meters per second on the y-axes and time on the x-axes, figures 45 and 48 respectively.

## 18 DC-motor

Actually, the system is not yet complete. Until this moment, just the pendulum and the cart have been taken into account, but the DC-motor should be implemented in the system as well. This is because the conveyor belt with the cart on it is driven by the DC-motor. Actually, the force acting on the cart is obtained from the torque of the motor. So, a rotational (motor) to linear (conveyor belt) translation takes place. In order to derive the expression for the torque, the electrical circuit of the DC-motor should be evaluated. In figure 4 already a picture with specifications of the motor used for this project is given.

There are four main types of DC-motors, the permanent magnet DC-motor, shunt wound DC-motor, the series wound DC-motor and the compound

wound DC-motor[20]. In an experiment the motor of this project is compared to a permanent magnet DC-motor. In this experiment the tension is measured when using the motor as a generator, which is equal to the back-emf generated in the rotor, for both the permanent magnet DC-motor and the motor used in this project. It turned out that the permanent magnet showed high tension when turning the shaft to which this motor is applied. This is due to the high back-emf, which is a characteristic of the permanent magnet DC-motor. After having applied the same experiment to the motor used in this project, it turned out there is no significant Voltage generated when trying to move the conveyor belt.

Considering the other three DC-motor types, the shunt DC-motor is able to maintain constant speed regardless of the load on the motor. This is because of the current through the series field coils[21], which are not there in a shunt DC-motor. Both figure 49 and 50 in the Appendix show the different relationships between the four types of DC-motors between speed and current or torque and current. Since there is not much data available for the motor used in this project, it cannot be easily concluded what type of motor it is. Therefore, to make a model just a basic circuit of a DC-motor is evaluated.

In figure 15 below a schematic of the circuit of a typical DC-motor with the corresponding variables is given, only in this case, as already explained, the motor used does not have or considerably small back-emf generated in the rotor. Therefore, in this case  $\epsilon$  can be neglected and only inductance and resistance are taken into account

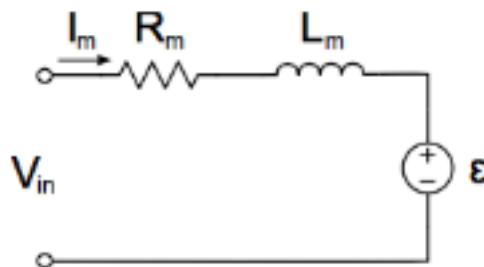


Fig. 15: Electrical circuit DC-motor[18]

- $V_{in}$  = the voltage applied to the motor (V)  
 $I_m$  = the current through the system (A)  
 $R_m$  = the ohmic resistance through the motor ( $\Omega$ )  
 $L_m$  = a coil that represents the inductance in the motor (H)  
 $\epsilon$  = the back-emf generated in the rotor  
 $k_m$  = the motor constant ( $\frac{Nm}{A}$ )  
 $\beta$  = the magnitude flux density (Wb)  
 $i$  = the current through the conductor (A)  
 $L$  = the length of the conductor (m)  
 $r$  = the mean radius of the motor (m)  
 $F$  = the force (N)  
 $T$  = the torque (Nm)  
 $d$  = the distance from the motor shaft to the belt (m)

From this circuit with the use of Kirchhoffs Voltage Law the following equations can be obtained[18]:

$$V_{in} = V_R + V_L \quad (79)$$

$$V_{in} = I_m R_m + L_m \frac{dI_m}{dt} \quad (80)$$

$$T = F * r = \beta * i * L * r = k_m * i \quad (81)$$

When substituting equation 81 in equation 80, equation 82 can be obtained. Thereafter, when applying Laplace transform to equation 82, equation 83 can be obtained, from which equation 84 is determined.

$$V_{in} = \frac{T}{k_m} R_m + \frac{L_m}{k_m} \frac{dT}{dt} \quad (82)$$

$$V_{in}(s) = \frac{T(s)}{k_m} R_m + \frac{L_m}{k_m} s T(s) \quad (83)$$

$$T(s) = \frac{V(s) k_m}{L_m s + R_m} \quad (84)$$

$$F = \frac{T}{d} \quad (85)$$

At last, the general formula for the force is given by equation 85, where  $d$  is the distance form the motor shaft to the belt, which from measurements turned out to be 0.022 meters. From these equations a model for the system with the force coming from the torque can be built in Simulink (figure 51). Figure 52 and 53 of the Appendix correspond to the subsystems of the complete system, where figure 53 denotes the model for the torque and

figure 52 the model for the force. Moreover, the values for  $k_m$ ,  $R_m$  and  $L_m$  should be obtained. The inductance ( $L_m$ ) and the ohmic resistance ( $R_m$ ) can be roughly estimated and theoretically assumed. In general, the value of the ohmic resistance of a DC-motor is assumed to be around  $4 \Omega$ , for the inductance this is  $0.072 \text{ Henry (H)}$  and for the motor constant this is  $1.26 \text{ V/rad/seconds}$  [25]. These are all generic values and can be neglected because this of minor influence on the complete system.

## 19 PID-controller

The first method to control the system is the use of a Proportional-Integral-Derivative (PID) controller. This controller captures the history of the system and anticipates future behavior. In general, the desired goals are a fast rise time, minimal overshoot and zero steady-state error. The rise time can be explained by the time taken by the output to change from 10 percent to 90 percent. The overshoot means the maximum percentage that the output exceeds the steady-state value, which is the output value of the system when time goes to infinity [16]. In figure 61 of the Appendix a schematic is given, in which these three points are explained in a scope.

In order to obtain the goals as mentioned, several steps have to be made. First, the open-loop response has to be obtained. Thereafter, it can be determined what needs to be improved. Then, a proportional controller can be added to improve the rise time, a derivative control to reduce the overshoot, and an integral control to reduce steady-state error ( $y_{ss}$ ). In figure 60 in the Appendix a clear overview of the type of controllers and its influence on the rise time and overshoot is given.

### 19.1 The angle of the pendulum

The transfer function of the angle of the pendulum is given by equation 36, defined as  $T_{pend}$ . This is the transfer function corresponding to the open-loop response. The general formula for the closed-loop response is given by equation 79, which can be clarified by figure 16 below. The general formula for the controller  $C(s)$  is given by equation 80.

$$G_1(s) = \frac{\theta(s)}{U(s)} = \frac{T_{pend}(s)}{1+C(s)T_{pend}(s)} \quad (79)$$

$$C(s) = k_p + \frac{K_i}{s} + k_d s \quad (80)$$

A script in Matlab can be written to obtain the right values for  $K_p, K_i, K_d$  denoted by figure 62 of the Appendix. At first, the angle of the pendulum is observed when  $K_p, K_i, K_d$  are all equal to -1 to which figure 63 in the Appendix corresponds. This is a minus number because the angle on the transfer function starts in the negative direction. It can be concluded, from this figure, that the rise time should be increased. Therefore, the value for  $K_p$  is increased to -120 (figure 64 of the Appendix). Now only the overshoot should still be reduced in order to obtain maximum overshoot of 0.05 radials, which is why the value for  $K_d$  becomes -30 (figure 65 of the Appendix). Since there is no difference between the integral controller being zero or minus one, this controller is decided to be equal to zero.

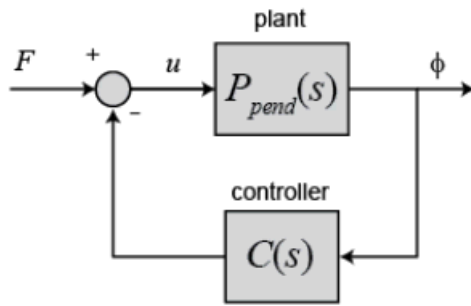


Fig. 16: Schematic PID-controller angle pendulum [17]

## 19.2 The position of the cart

After having designed the PID-controller for the angle of the pendulum, the influence on the position of the cart can be analyzed. The open-loop transfer function corresponding to the position of the cart is denoted by  $T_{cart}$  (equation 37). Figure 17 shows the closed-loop transfer function for the position of the cart. This can then be modelled in Matlab (figure 62 of the Appendix) of which the result is given in figure 66 of the Appendix. It can be concluded, from this figure, that the position is not yet stable because it still goes to infinity.

$$G_2(s) = \frac{T_{cart}(s)}{1+T_{pend}(s)C(s)} \quad (81)$$

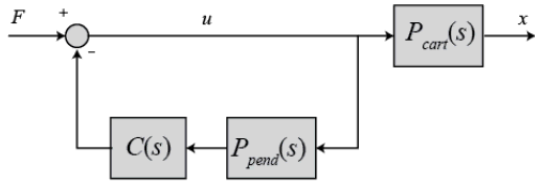


Fig. 17: Schematic PID-controller position cart with feedback [17]

## 20 PID in Simulink

The PID-controller in matlab can also be tested in Simulink by making a model (figure 71 of the Appendix). It can be concluded from the scopes (figures 67 and 68 of the Appendix) that the PID-controller is correct since the angle will go back to zero in around one second. The position will still go to infinity and is therefore not yet controlled.

Now, this controller can be implemented in the Simulink model with connection blocks to read the position and the angle (figure 12). In figure 2 already a global overview of the system from PC to potentio-meter and encoder is given. Below in figure 18 a more detailed version of this can be found. There are two streams coming into the target hard-ware platform, one from the ADC block corresponding to the potentio-meter and one from the encoder. There is also one stream going out of the target hard-ware platform to the amplifier, which powers the motor. With a digital to analogue (DAC) block in Simulink, the data from the PC is communicated to the analogue to digital (ADC) block and the encoder block. The plant as shown in figure 2 is external. In figure 69 and 70 of the Appendix a schematic overview of this is given.

The PID in the model of figure 72 is in discrete-time. The controller already determined is in continuous-time and therefore has to be translated to discrete-time, to check if the determined controller is correct. In equation 82 below the discretized version of the formula for the controller is given. The forward-euler method is applied in this case (equation 83). When comparing the discrete and continuous versions of the formula for the controller, equations 84, 85 and 86 can be obtained, from which it can be concluded that both the derivative and integral controller are influenced by the sam-

ple time. Since the integral controller is defined as zero for the continuous PID-controller, this value stays the same for the discrete PID-controller. Besides this, the proportional controller will also remain the same because it is not influenced by the sample time in the discrete PID-controller. Only, the discrete derivative controller might deviate from the continuous derivative controller, but after testing this on the pendulum in its vertical downwards position it turned out that the discrete PID controller with the same values as the continuous PID-controller is appropriate.

$$C(z) = K_p + K_d \frac{z-1}{T} + \frac{K_i T}{z-1} \quad (82)$$

$$s = \frac{z-1}{T} \quad (83)$$

$$P_z = K_p \quad (84)$$

$$D_z = K_d \frac{z-1}{T} \quad (85)$$

$$I_z = \frac{K_i T}{z-1} \quad (86)$$

## 21 Testing Inverted Pendulum

At first, it is significant to get a clear overview of the interconnections between the computer and the plant. A detailed version of this is given in figure 18 below. It can be concluded, from this figure, that the inputs of the target hardware platform are the streams of the ADC-board and the encoder. The output is the stream going to the amplifier communicated by the DAC-board.

In order to test if the controller is appropriate for the pendulum in its upwards vertical position (Inverted Pendulum) as well, first boundaries for the transport rail have to be added in order to make testing more safe. These boundaries mean that the cart will stop when reaching a certain position. This can be obtained by introducing a switch into the model of figure 72. This switch implies that when the position is in between -6000 and 6000 pulses, there will still be voltage applied. Actually, when the position is outside the boundaries, the voltage will go to zero, the DAC block will send a signal of zero voltage to the amplifier by which the motor will stop and therefore also the transport rail will stop. In figure 73 of the Appendix a schematic of this model in Simulink is given.

Since there are boundaries included, the inverted pendulum can be tested. After the first test, it turned out that the controller designed is not fast enough since the cart is not able to adjust fast enough to stabilize the inverted pendulum. To solve this problem the derivative controller is increased to 200 in order to decrease the settling time. Moreover, the proportional and integral controller are increased by 200 and 3 respectively to decrease the rise time. Lastly, also the sample time is decreased to 0.005 seconds. At these conditions, the inverted pendulum seems to be stabilized for one side only and will still go to infinity. This is because the position of the cart is not yet controlled by the designed PID-controller, which was already concluded from the simulations.

The position of the cart is dependent on the angle of the pendulum. Because of this, the position of the cart can be controlled by adding an offset to the angle measurement that is proportional to the position of the cart. So, the position of the cart is multiplied by a gain of -0.000005 and given as offset to the angle measurement. Moreover, a derivative controller is added to the offset of the angle measurement. By adding the derivative controller, the cart will tend to go the center point even faster. Figure 77 of the Appendix gives a clear overview of the corresponding model in Simulink. When testing this, it turned out that the values of the PID-controller had to be adjusted, which is a logic response since the position of the cart is used as offset. The optimal value for  $K_p$  is 1000 and for  $K_d$  1800, the integral controller is zero. The cart now tends to go to the center of the transport rail due to the angle of the pendulum and is therefore controlled. These values for the PID-controller cannot be compared to the simulations, since there are no converters included in the model of figure 77 and the offset added to the angle of the pendulum is in pulses of the position.

Actually, now the control system is optimal but there occurred some resonance in the aluminium pendulum, which disturbs the stabilization of the inverted pendulum. In order to avoid this resonance, different material for the inverted pendulum should be used, which is in this case plastic. Moreover, the pendulum should be hollow to avoid resonance. Figure 78 of the Appendix shows a picture of the plastic pendulum used with a certain weight on it. When testing with this inverted pendulum, no resonance occurred any-

more and the inverted pendulum was stabilized around its vertical upwards position while the cart tends to go to the center of the transport rail. Only, after every stabilization the cart takes more space on the transport rail to stabilize. Therefore, it can be concluded that the control system in this case is not optimal. In order to find out where this problem exactly is coming from, a new model has to be made considering this inverted pendulum.

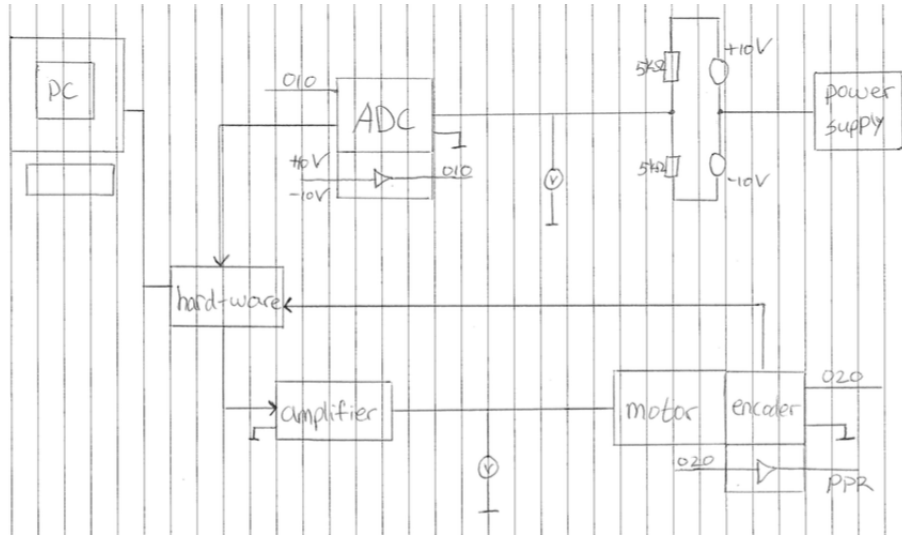


Fig. 18: Detailed version of the system from PC to potentio-meter and encoder

## 22 Conclusion

To conclude, the main research question is answered. This is because the two requirements of keeping the pendulum in its vertical upwards position and to keep the cart around the center of the transport rail are succeeded.

At first, mathematical modelling is applied to obtain the equations of motion and thereby obtain an answer to the second sub research question. Thereafter, the equations for the transfer functions and the state-space equations are obtained (sub question 3), after which these equations are all modelled in Simulink from which it is concluded that the equations are correct (sub question 4). Since there were still some unknown variables corresponding to the system, these variables were either obtained or determined corresponding to sub question 5. One of these unknown variables is the length of the

pendulum, which is chosen to be as long as possible because this makes it easier to control (sub question 1). Moreover, the potentio-meter and the encoder were significant to analyze, from which it can be concluded that the the potentio-meter shows Voltage on the y-axes of the scopes of the angle, and the encoder shows pulses on the y-axes of the scopes of the position of the cart. It is more clear to read the angle in degrees from the y-axes and the position in meters per second. This translation of y-axes is obtained through experiments for the angle of the pendulum and through measurements for the position of the cart by which the diameter of the pulley of the transport rail is a significant constant used (sub question 8). Since the force on the cart is coming from the torque of the motor, the DC-motor is analyzed. Through testing it turned out that the DC-motor used in this project is not a permanent-magnet DC-motor, but it is hard to define what type of DC-motor it actually is due to lack of data about the specific DC-motor of the project and its complexity. Therefore, a model in Simulink is build considering the basic circuit of a DC-motor.

In order to obtain a more specific overview of the complete system and the connection between the computer and the plant, different schematics are obtained. To obtain the goal of stabilizing the inverted pendulum, a PID-controller is designed. The PID controller designed is appropriate for the pendulum in its vertical downwards position. Actually, for the pendulum in its vertical upwards position, the PID-controller is adjusted in order to be fast enough. From simulations it can be concluded that the position of the cart is not yet stabilized by this PID-controller. Therefore, boundaries for the transport rail are added to make testing more safe, which answers sub question 6 of the research questions. In order to solve this problem, a controller for the position of the cart had to be added. This is done by adding an offset to the angle measurement that is proportional to the position of the cart. Moreover, a derivative controller is added to the offset of the angle measurement. The combination of this provides optimal stabilization of the inverted pendulum around its vertical upwards position while the cart tends to go to the center of the transport rail. This gives an answer to sub question 9, that the target-hardware platform is indeed fast enough in computations per seconds for the Inverted Pendulum using a sample time of 0.005. From testing, it is concluded that there is resonance in the alu-

minium inverted pendulum, which disturbs the stabilization of the inverted pendulum. Another hollow inverted pendulum, with plastic as material and a certain weight at the top is used to remove resonance in the inverted pendulum. There is no resonance anymore, but from testing it is concluded that the stabilization of the inverted pendulum is less optimal under the same conditions compared to the first inverted pendulum used.

So, in the end it can be concluded that with the models and controllers obtained there are two options. The first option is, that the first aluminium inverted pendulum is used, corresponding to all the models obtained, by which the control system is optimal but there is resonance in the pendulum, which disturbs the stabilization of the inverted pendulum. The second option is, that the hollow plastic inverted pendulum is used with the certain weight on top, where the resonance is removed, but the control system is not optimal.

## 23 Discussion

The requirements to keep the inverted pendulum around its vertical upwards position and the cart around the center position of the transport rail are satisfied. Only an unexpected disturbance occurred, the resonance in the aluminium inverted pendulum. Since it cannot easily be concluded where this resonance in the system is coming from, a plastic pendulum with a certain weight on it is tested on the system. With this pendulum the weight is on the end of the pendulum, while the weight of the aluminium pendulum is considered to be around the center of the pendulum. Therefore, actually for the plastic pendulum different models have to be obtained. This can also be concluded from the fact that the control system is not optimal under the same conditions for the hollow, plastic pendulum compared to the system with the aluminium inverted pendulum. So, for further research it could either be examined where in the system the resonance is coming from. When the resonance is removed, the optimal control system with the aluminium inverted pendulum could be used. Another option is to obtain the new models corresponding to the hollow, plastic inverted pendulum with the weight at the end of the pendulum. This way the values for the PID-controller corresponding to this inverted pendulum can be obtained and probably converters have to be added in the Simulink model of figure 77 to

be able to compare it to the models created. The latter option is probably more feasible, since it is really complex to find where in the system exactly the resonance is coming from.

Furthermore, further research to the DC-motor used in this project could be done. It is complex to conclude what type of DC-motor is used, but through experiments by for example measuring the angular velocity, it could become more clear what type of DC-motor exactly is used. Besides this, also the motor constant and the ohmic resistance can be obtained through experiments. In this report just the general values are used, since these values are of minor influence compared to the overall system and the mechanical part of the system in specific.

Lastly, besides a PID-controller also a model-based controller can be designed, but this was not feasible within the given time frame, as already mentioned in the risk and feasibility section of the report. The advantage of a model-based controller compared to a PID-controller is that when designing a model-based controller probably both the angle of the pendulum and the position of the cart are controlled using one controller, where with the PID-controller two separate controllers have to be used.

## 24 Appendix

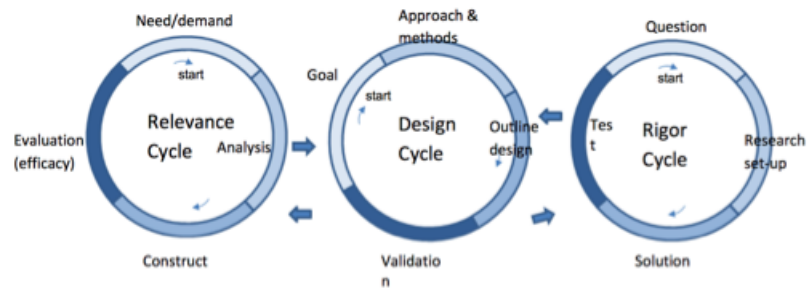


Fig. 19: Cycles of Hevner[8]

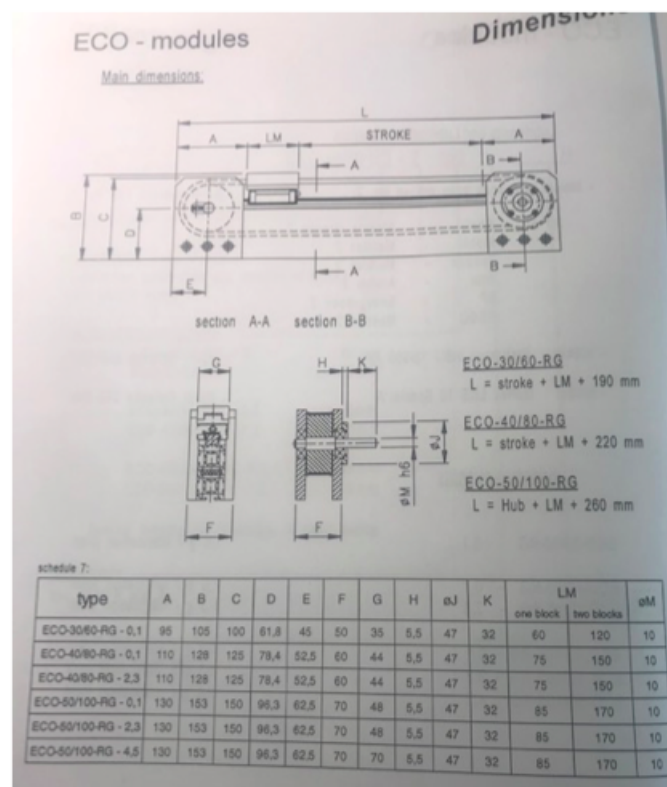


Fig. 20: Transport rail information [3]

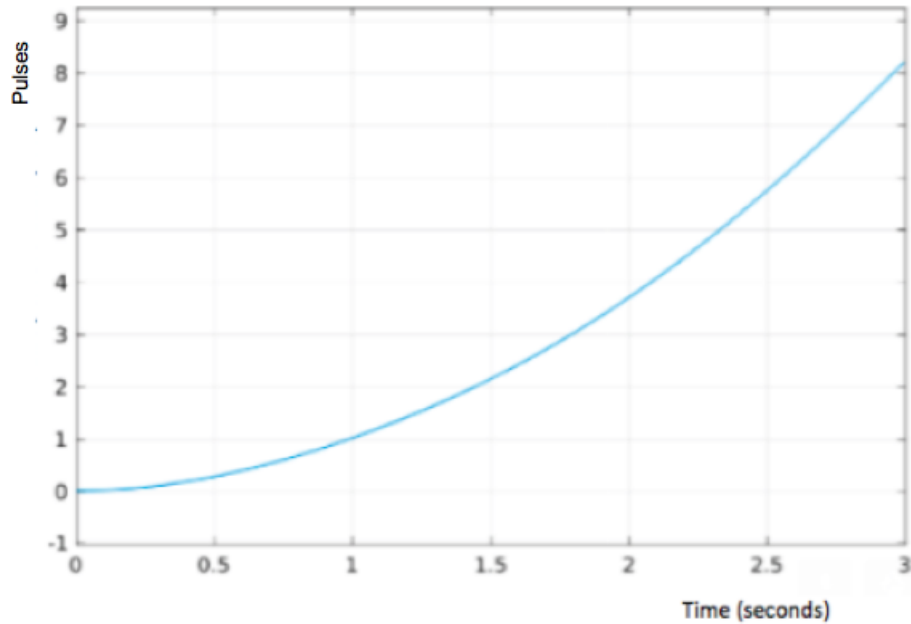


Fig. 21: Scope of the position of the cart  $t=3$

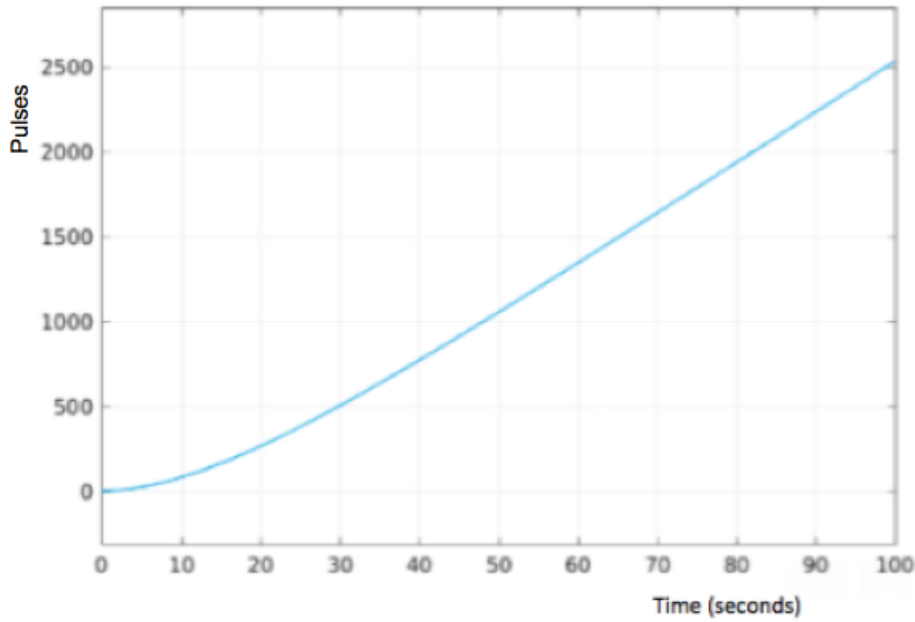


Fig. 22: Scope of the position of the cart  $t=100$

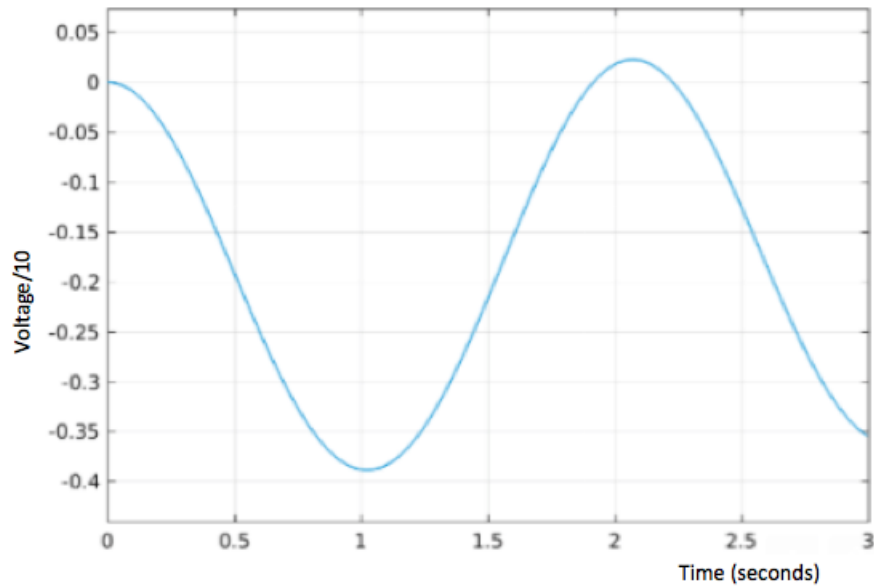


Fig. 23: Scope of the angle of the pendulum  $t=3$

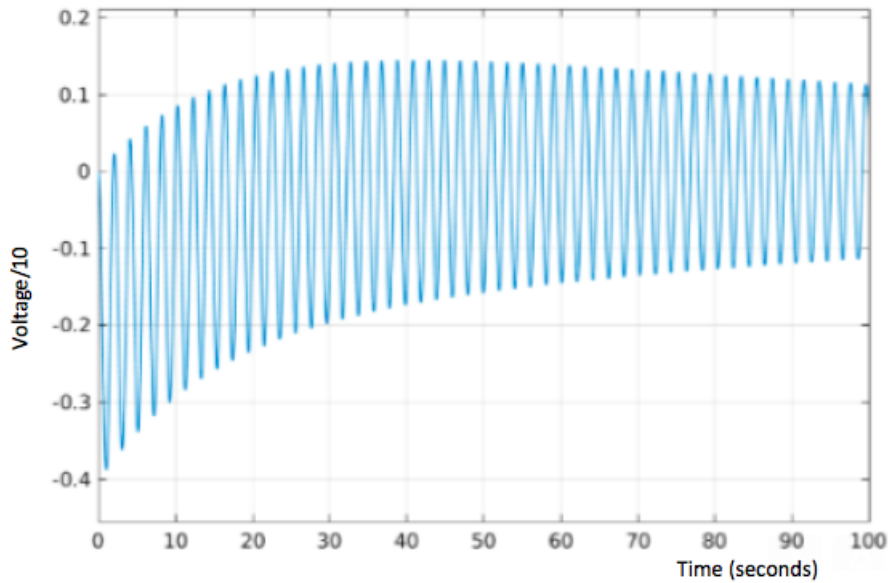


Fig. 24: Scope of the angle of the pendulum  $t=100$

```
M = 1.2414;
m = 0.31;
b = 0.1;
I = 0.082;
g = 9.81;
l = 0.89;
q = (M+m) * (I+m*l^2) - (m*l)^2;
s = tf('s');

T_cart = ((m*l^2+I)*s^2+g*m*l/q)/(s^4+(b*(m*l+I)/q)*s^3+((M+m)*g*m*l/q)*s^2+(b*m*g*l/q)*s);
T_pend = (-m*l*s/q)/(s^3+(b*(m*l^2+I)/q)*s^2+((M+m)*g*m*l/q)*s+(b*m*g*l/q));

sys_tf = [T_cart ; T_pend];

inputs = {'u'};
outputs = {'x'; 'theta'};

set(sys_tf, 'InputName', inputs)
set(sys_tf, 'OutputName', outputs)

t=0:0.01:1;
impulse(sys_tf,t);
title('Open-Loop Impulse Response')
```

Fig. 25: matlab transfer function

```

M = 1.2414;
m = 0.31;
b = 0.1;
I = 0.082;
g = 9.81;
l = 0.89;

p = I*(M+m)+(M*m*l^2); %denominator for the A and B matrices

A = [0 1 0 0;
      0 -(I+m*l^2)*b/p (m^2*g*l^2)/p 0;
      0 0 0 1;
      0 (m*l*b)/p -m*g*l*(M+m)/p 0];
B = [0;
      (I+m*l^2)/p;
      0;
      -m*l/p];
C = [1 0 0 0;
      0 0 1 0];
D = [0;
      0];

states0 = {'x' 'x_dot' 'theta' 'theta_dot'};
states1 = {'x'};
states2 = {'x_dot'};
states3 = {'theta'};
states4 = {'theta_dot'};
inputs = {'u'};
outputs = {'x'; 'theta'};
```

Fig. 26: matlab state-space

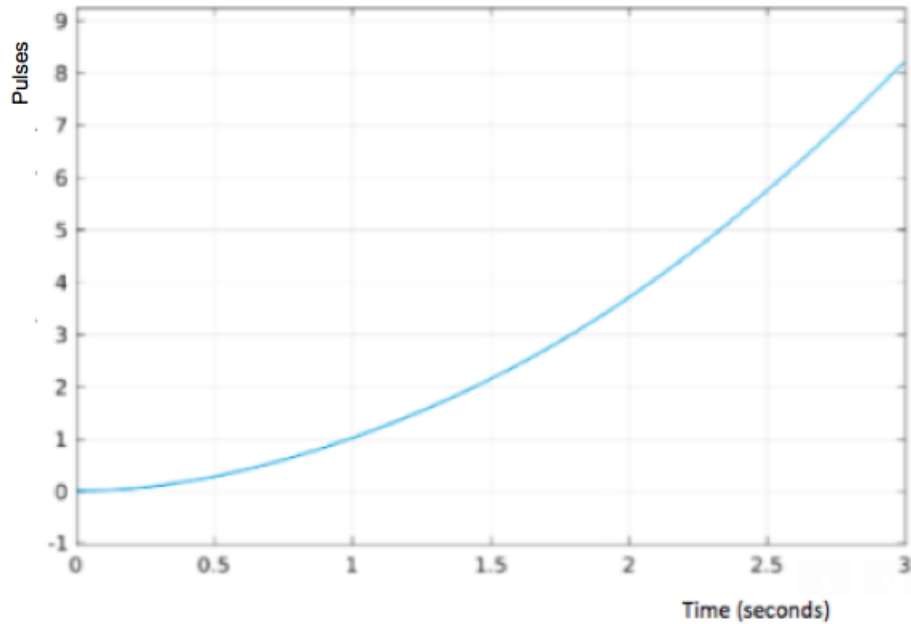


Fig. 27: Scope of transfer function: position,  $t=3$

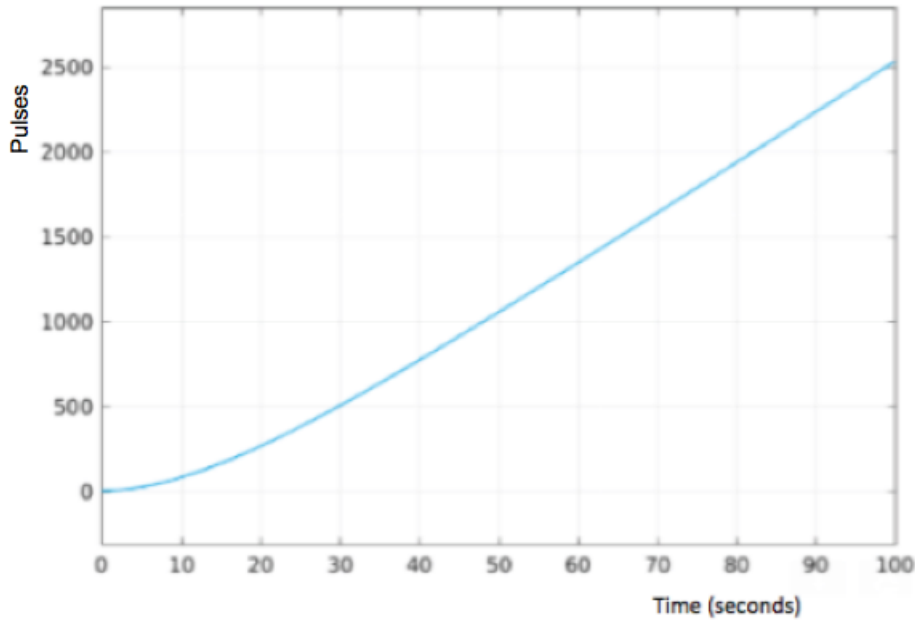


Fig. 28: Scope of transfer function: position,  $t=100$

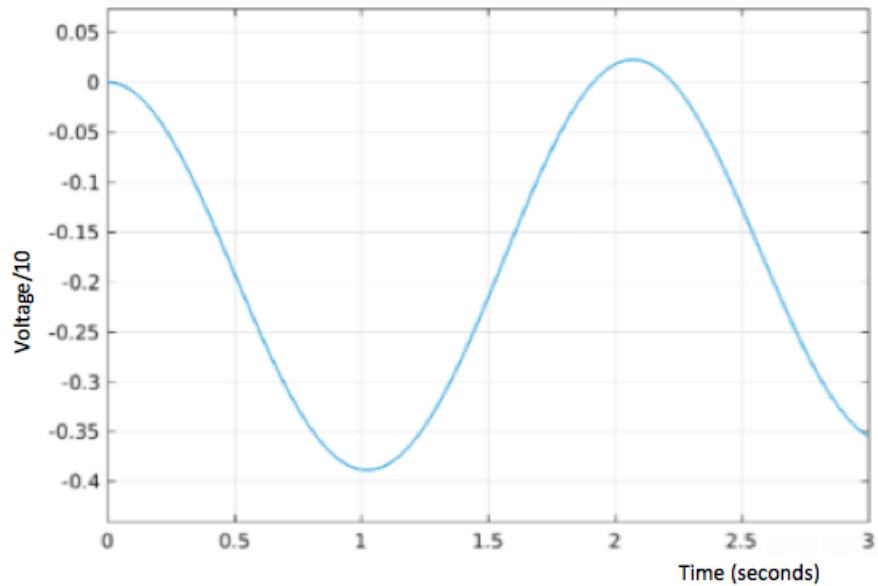


Fig. 29: Scope of transfer function: angle,  $t=3$

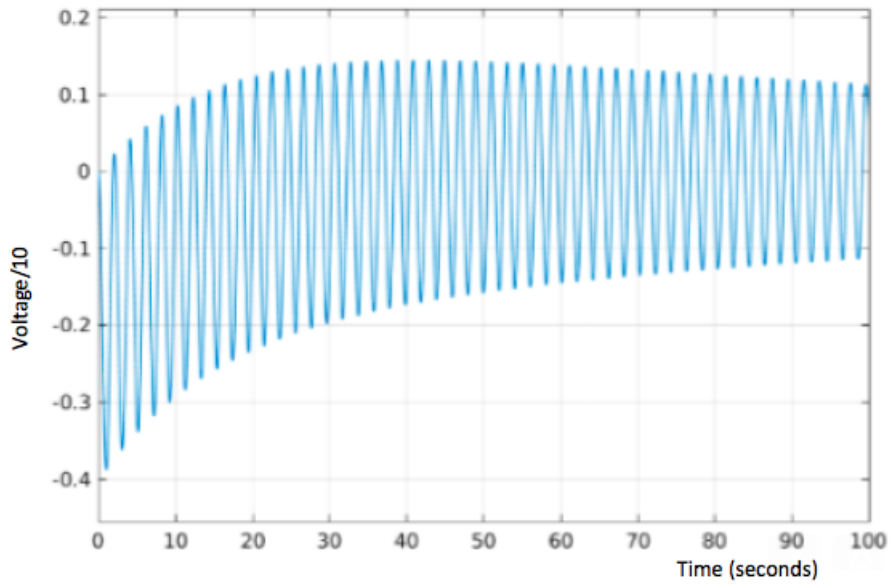


Fig. 30: Scope of transfer function: position,  $t=100$

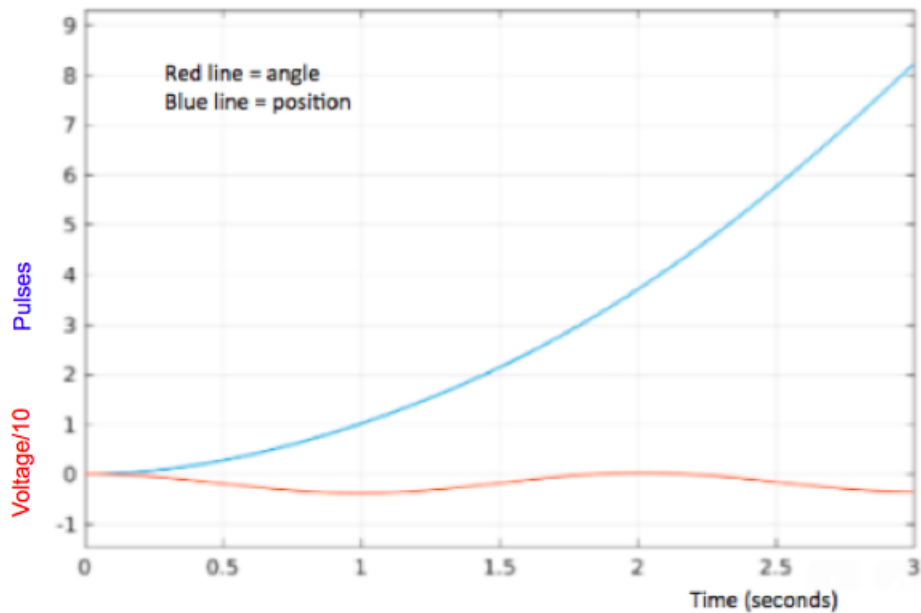


Fig. 31: Scope of state-space at  $t=3$

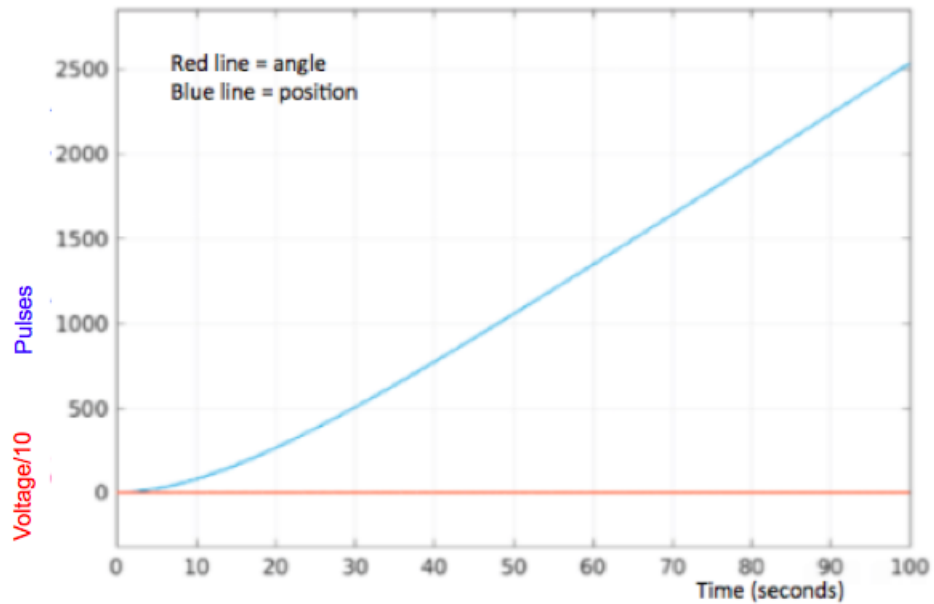


Fig. 32: Scope of state-space at  $t=100$

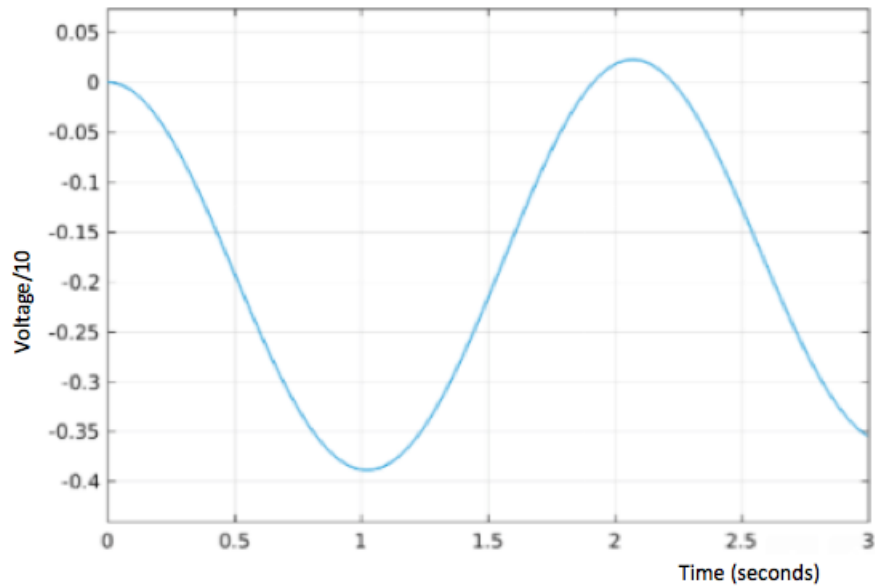


Fig. 33: Scope of state-space at  $t=3$  zoomed in

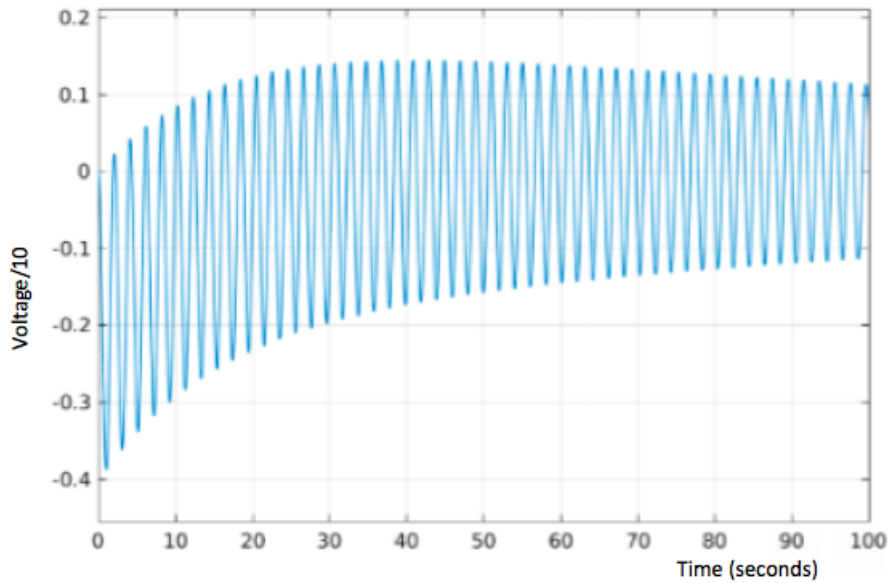


Fig. 34: Scope of state-space at  $t=100$  zoomed in



Fig. 35: Potentio-meter

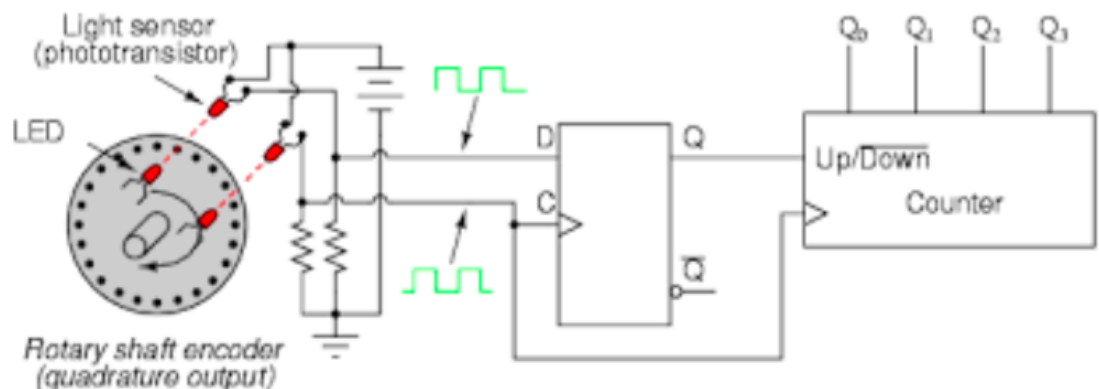


Fig. 36: Schematic encoder [18]

Phase	A	B
1	0	0
2	0	1
3	1	1
4	1	0

Fig. 37: Table of the direction of the encoder [13]

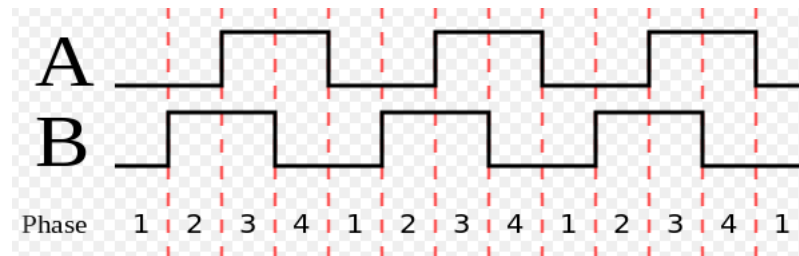


Fig. 38: Schematic function of the encoder [13]

```

x = [-0.5 -0.4 -0.3 -0.22 -0.18 -0.05 0 0.05 0.18 0.22 0.3 0.4 0.5];
y = -90:15:90;
n = 1;
p = polyfit(x,y,n)

xfit = [-0.6:1:0.6];
yfit = p(1)*xfit+p(2);
plot(xfit,yfit,x,y, 'ro')
xlabel('Output Voltage/10')
ylabel('Angular position (degrees)')
legend('fitted curve', 'recorded data', 'Location', 'NorthWest')
text(0,-80,'y = 186.9535x + 0')

%plot(angle.time, p(1)*angle.signals.values+p(2))

```

Fig. 39: Matlab script of graph angle of the pendulum

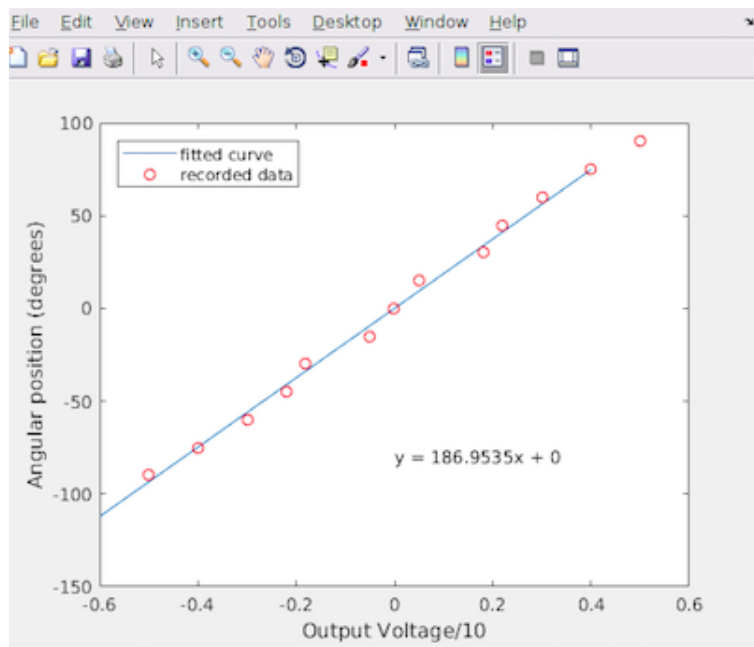


Fig. 40: Graph Voltage to degrees of the angle

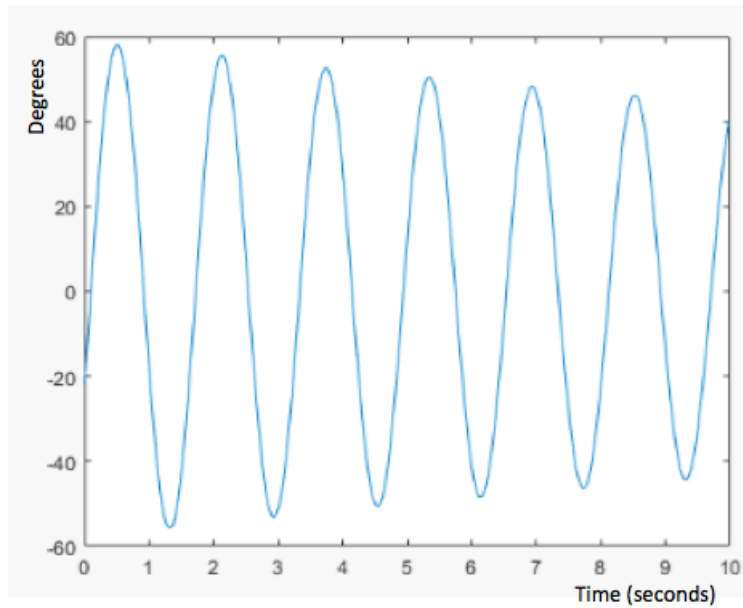


Fig. 41: Graph time to degrees for smaller angles

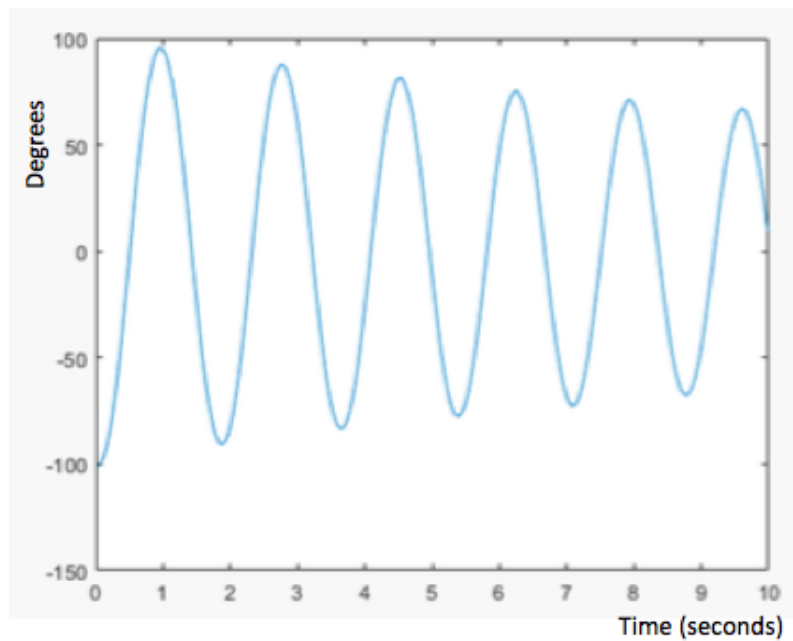


Fig. 42: Graph time and degrees for bigger angles

```

x = -6000:2000:6000
y = [-62 -42 -28 0 28 42 62];
n = 1;
p = polyfit(x,y,n)

xfit = [-6000:1:6000];
yfit = p(1)*xfit+p(2);
plot(xfit,yfit,x,y, 'ro')
xlabel('Counts')
ylabel('Centimeters')
legend('fitted curve 0.0106x + 0')

plot(ScopeData2.time, p(1)*ScopeData2.signals(2).values+p(2))
xlabel('time')
ylabel('Centimeters')

```

Fig. 43: Matlab script graph position cart

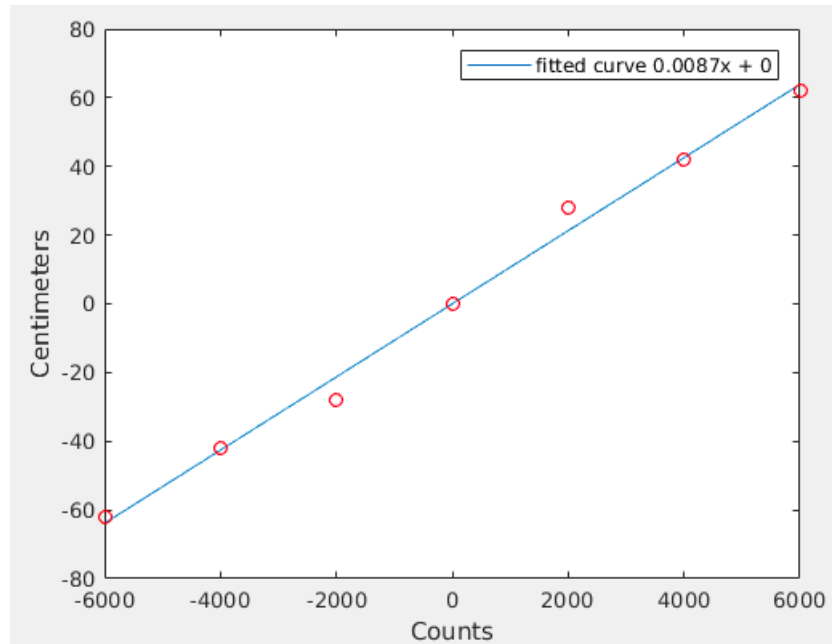


Fig. 44: Centimeters to counts of the position of the cart

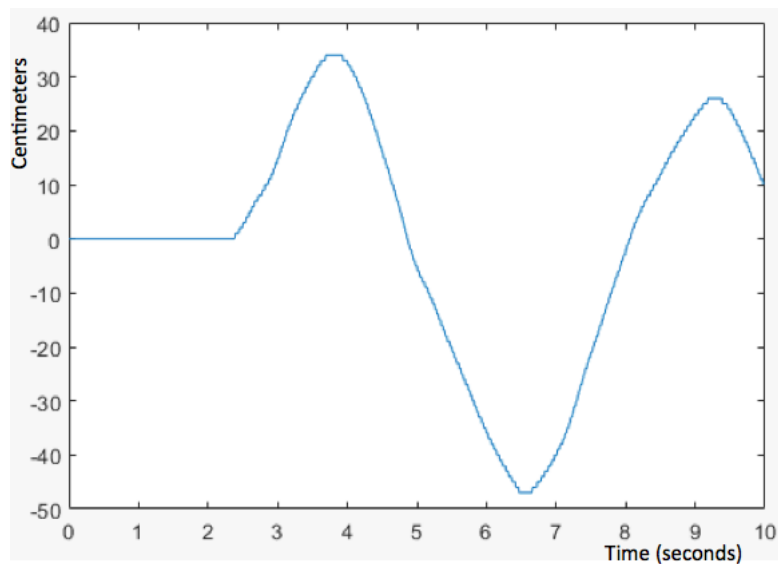


Fig. 45: Centimeters to time of the position of the cart

```
x = -30:10:30;
y = [-31.2 -20.8 -10.4 0 10.4 20.8 31.2];
n = 1;
p = polyfit(x,y,n);

xfit = -30:1:30;
yfit = p(1)*xfit+p(2);
plot(xfit,yfit,x,y, 'ro')
xlabel('Counts per sample period')
ylabel('Centimeters per second')
legend('fitted curve', 'recorded data','Location','NorthWest')
text(10,-0.03, 'y = 1.04x + 0')

%plot(ScopeData2.time, p(1)*ScopeData2.signals(1).values+p(2))
```

Fig. 46: Matlab script graph speed cart

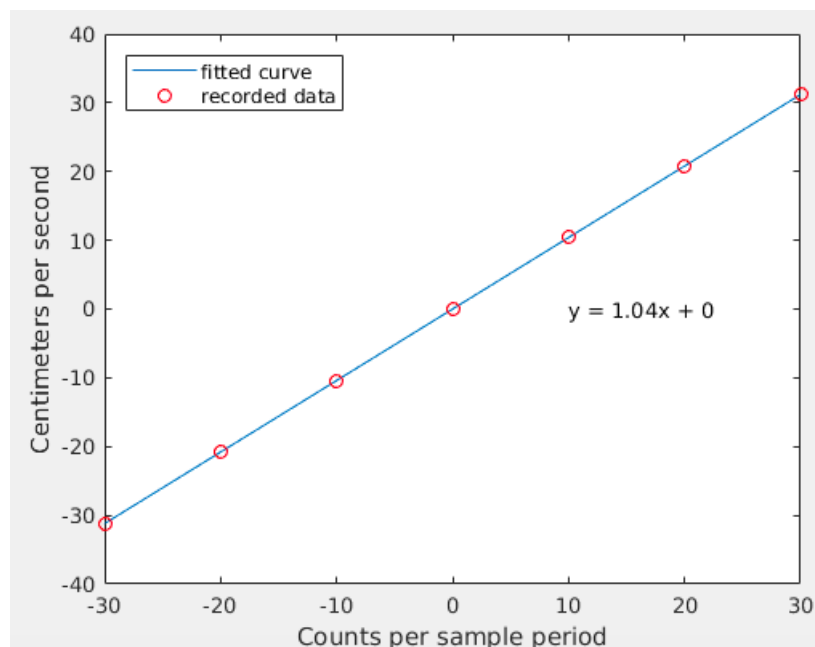


Fig. 47: Centimeters to counts per sample period of the speed of the cart

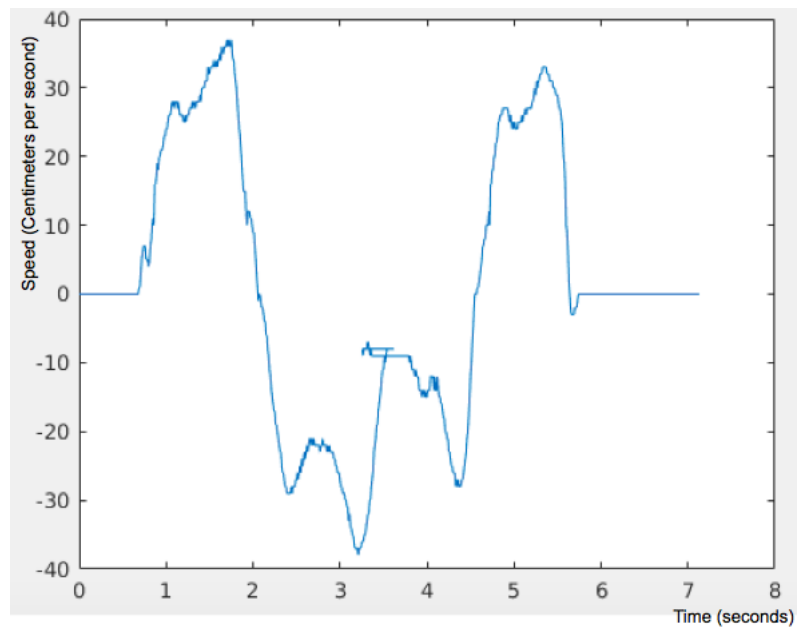


Fig. 48: Centimeters per second to time in seconds of the speed of the cart

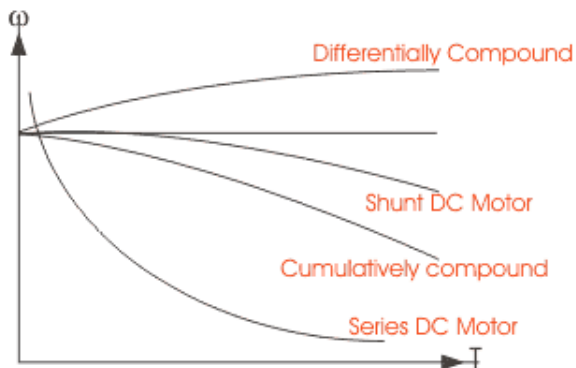


Fig. 49: Torque and angular speed [20]

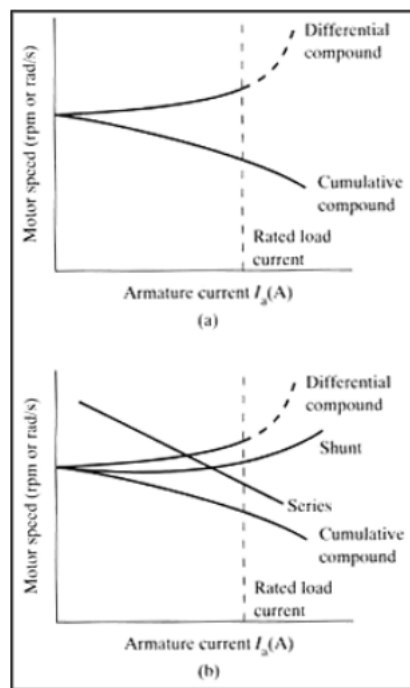


Fig. 50: Motor speed and armature current [23]

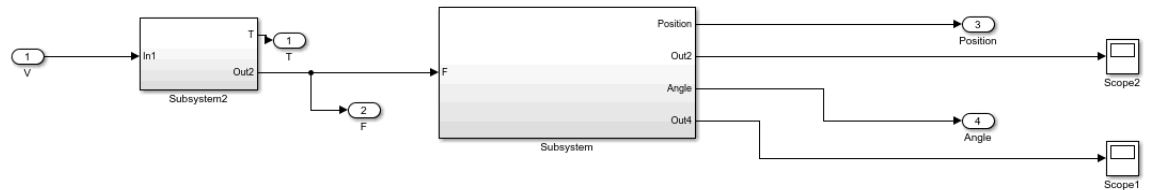


Fig. 51: The system with the torque coming from the force

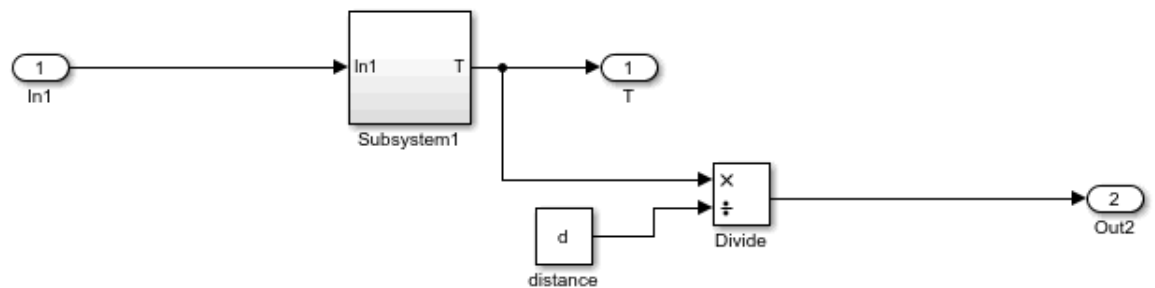


Fig. 52: Sub system 2

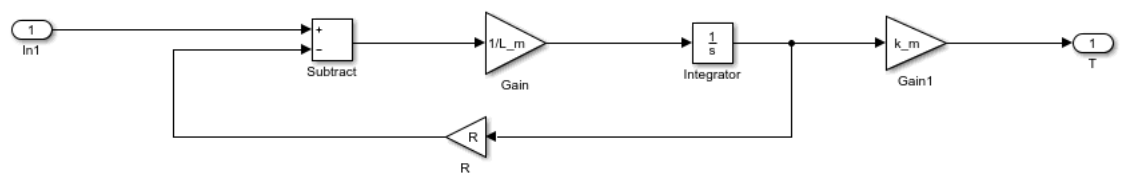
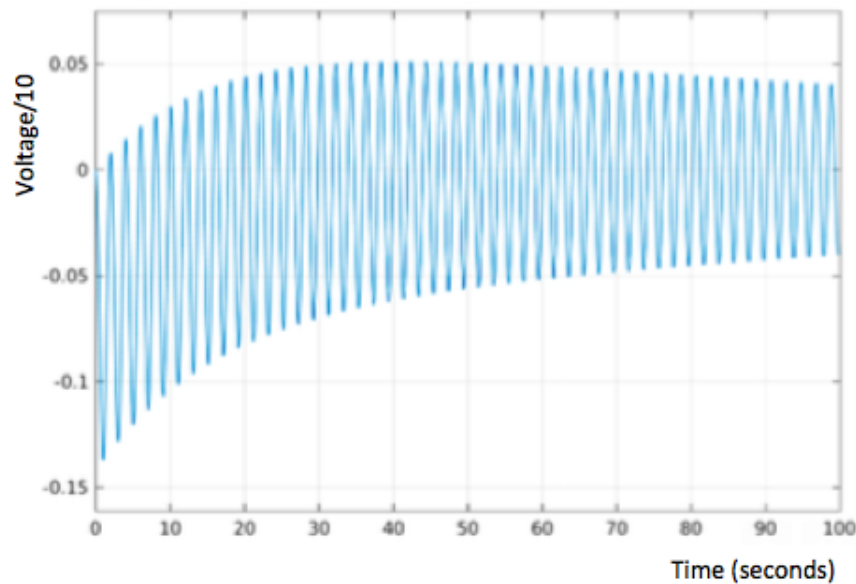


Fig. 53: Sub system 1

Fig. 54: Angle of the pendulum of complete system at  $t=100$

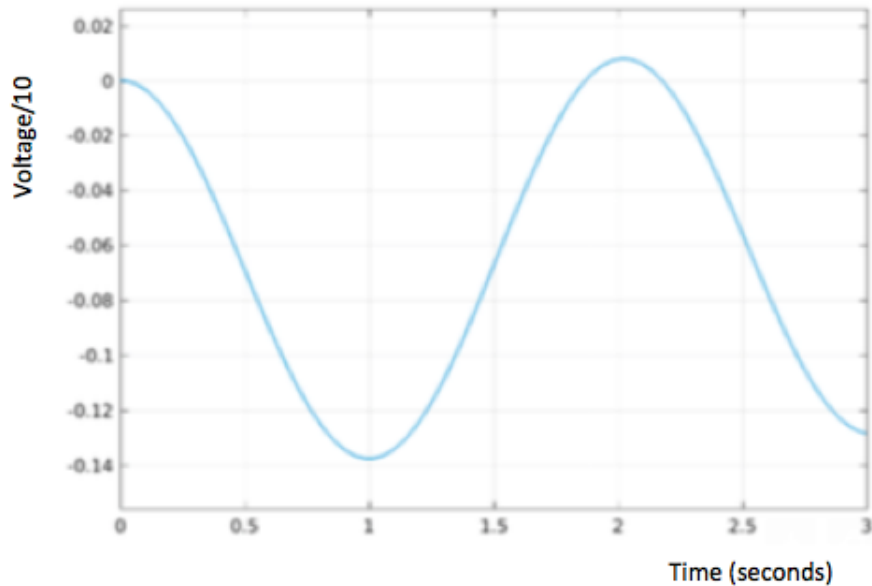


Fig. 55: Angle of the pendulum of complete system at  $t=3$

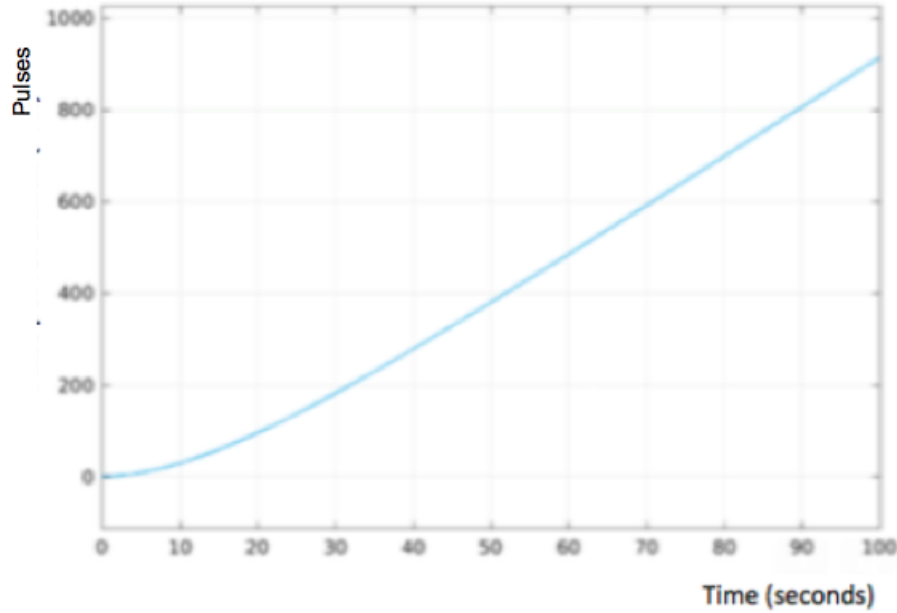


Fig. 56: Position of the cart of complete system at  $t=100$

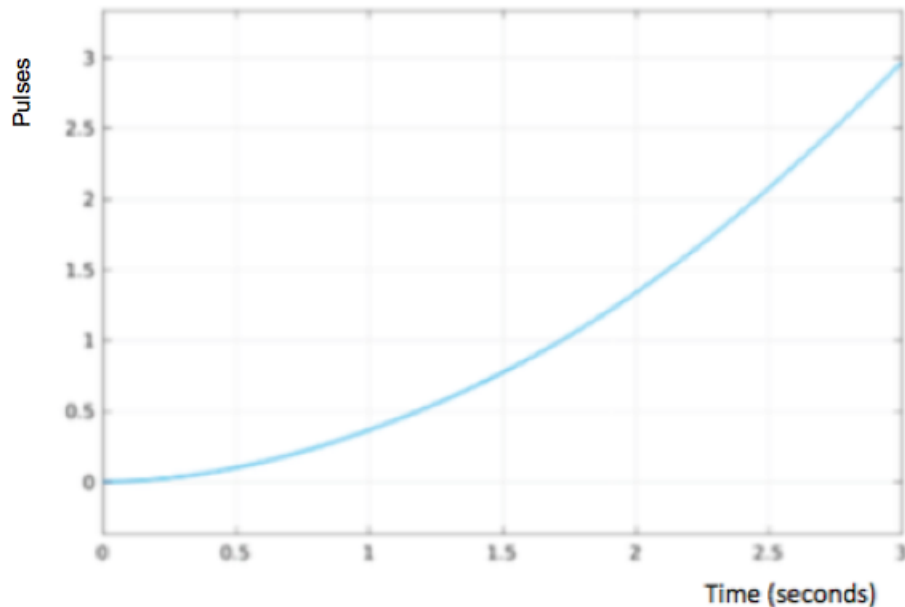


Fig. 57: Position of the cart of complete system at  $t=3$

```
x = 0:0.5:3
y = [2.46 2.56 2.64 2.7 2.77 2.8 2.82];
n = 1;
p = polyfit(x,y,n)

xfit = [0:1:3];
yfit = p(1)*xfit+p(2);
plot(xfit,yfit,x,y, 'ro')
xlabel('Current (A)')
ylabel('Force (N)')
legend('fitted curve', 'recorded data','Location','NorthWest')
text(200,-0.1, 'y = 0.0433x + 2.6238')
```

Fig. 58: Matlab script of the relation between current and force

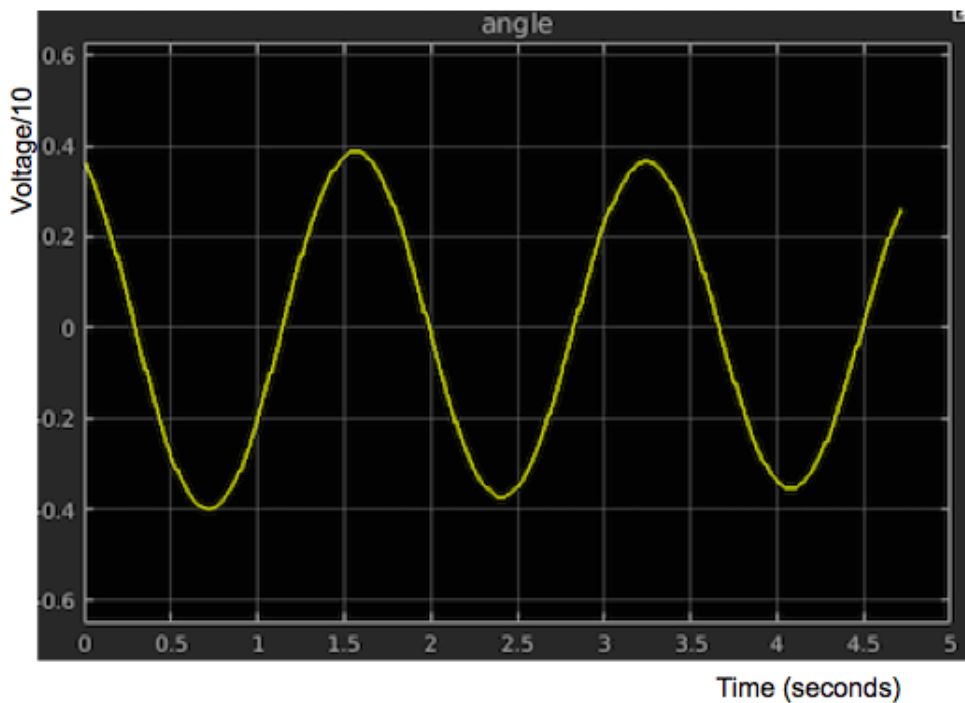


Fig. 59: Scope of the angle from Simulink

CL RESPONSE	RISE TIME	OVERSHOOT	SETTLING TIME
K <sub>p</sub>	Decrease	Increase	Small Change
K <sub>i</sub>	Decrease	Increase	Increase
K <sub>d</sub>	Small Change	Decrease	Decrease

Fig. 60: Influence of PID-controllers on rise time, overshoot and settling time  
[17]

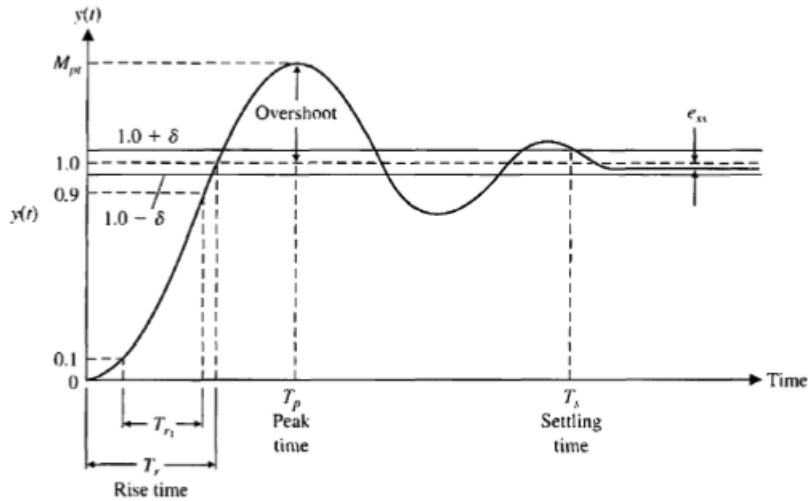


Fig. 61: Schematic of rise time, overshoot, steady-state [16]

```

M = 1.2414;
m = 0.31;
b = 0.1;
I = 0.082;
g = 9.81;
l = 0.89;
q = (M+m) * (I+m*l^2)-(m*l)^2;
s = tf('s');

T_pend = (-m*l*s/q)/(s^3+(b*(m*l^2+I)/q)*s^2+((M+m)*g*m*l/q)*s+(b*m*g*l/q));

kp = -120;
ki = 0;
kd = -30;
C = pid(kp,ki,kd);
G = feedback(T_pend,C);

t = 0:0.01:2;
impulse(G,t)
title({'response of pendulum position to an impulse disturbance';'under PID control: kp=-120, ki=-1, kd=-30'});

%T_cart = ((m*l^2+I)*s^2+g*m*l/q)/(s^4+(b*(m*l+I)/q)*s^3+((M+m)*g*m*l/q)*s^2+(b*m*g*l/q)*s;
%G2 = feedback(1, T_pend*C)*T_cart;
%t = 0:0.01:5;
%impulse(G2,t)
%title({'response of position of cart to an impulse disturbance';'under PID control: kp=-120, ki=-1, kd=-30'})

```

Fig. 62: Matlab script PID

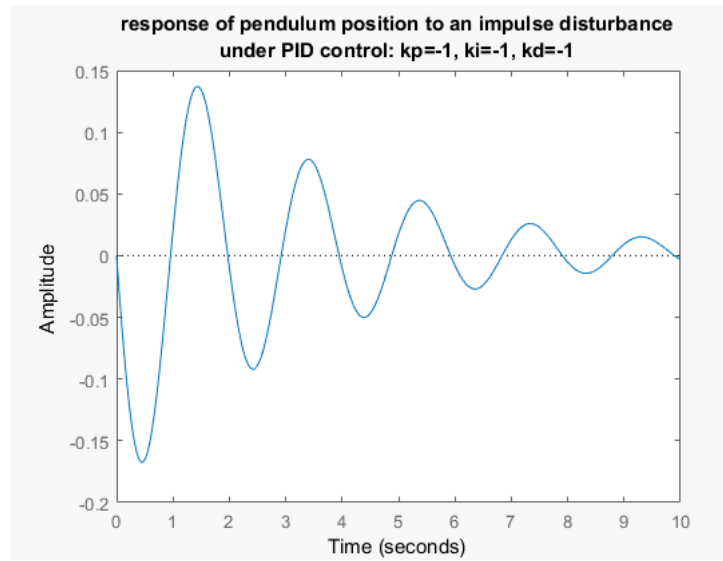


Fig. 63: The angle of the pendulum under PID control:  $K_p = -1, K_i = -1, K_d = -1$

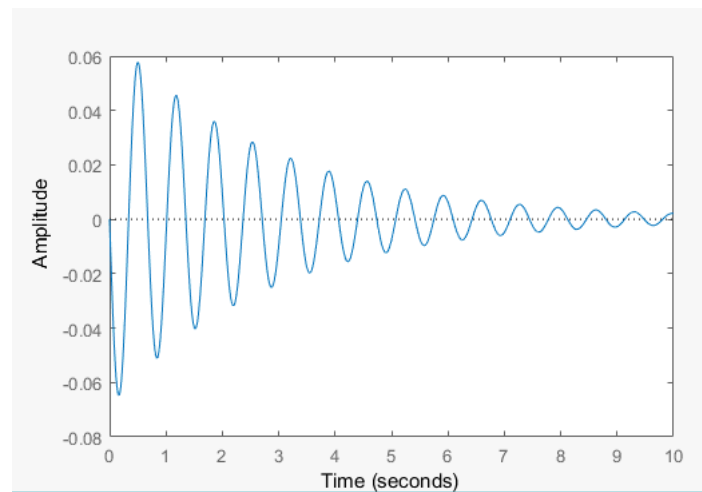


Fig. 64: The angle of the pendulum under PID control:  $K_p = -120, K_i = -1, K_d = -1$

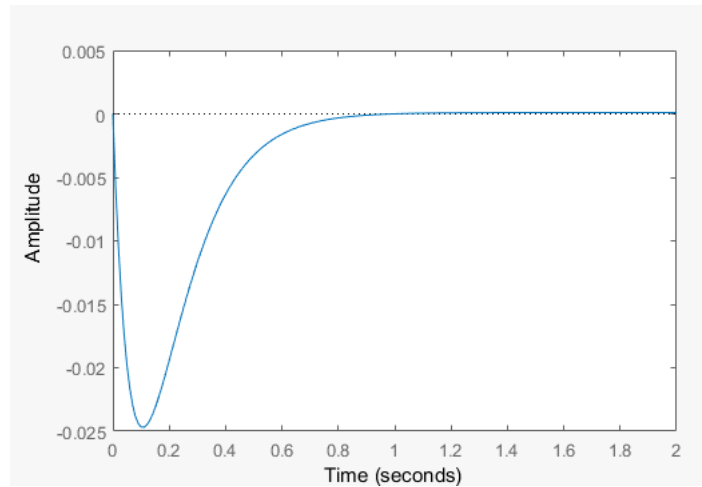


Fig. 65: The angle of the pendulum under PID control:  $K_p = -120, K_i = -1, K_d = -30$

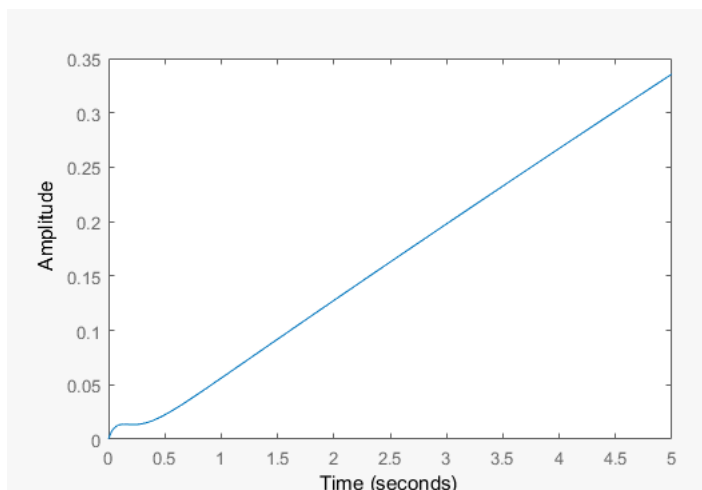


Fig. 66: The position of the cart under PID control:  $K_p = -120, K_i = -1, K_d = -30$

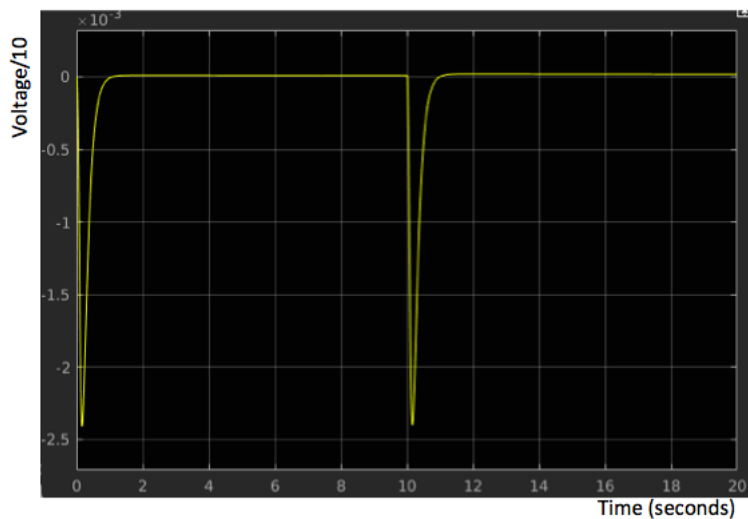


Fig. 67: Scope of the angle of model ...

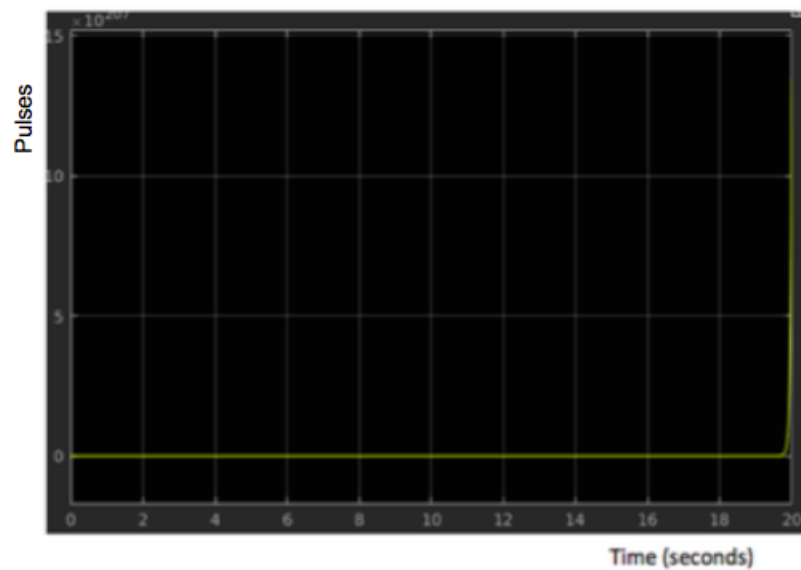


Fig. 68: Scope of the position of model 71

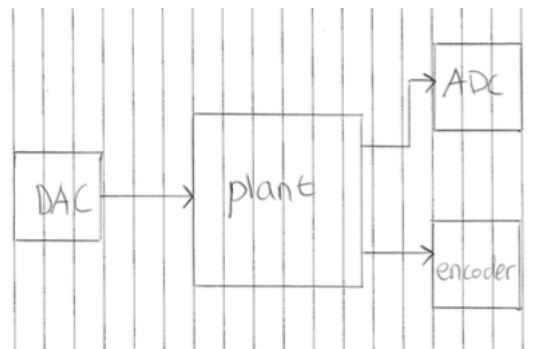


Fig. 69: Overview communication from the computer to connection blocks of the position and the angle

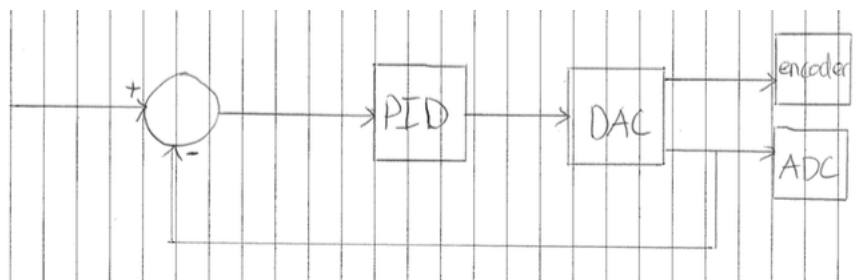


Fig. 70: Overview communication from the computer to connection blocks of the position and the angle with PID-controller

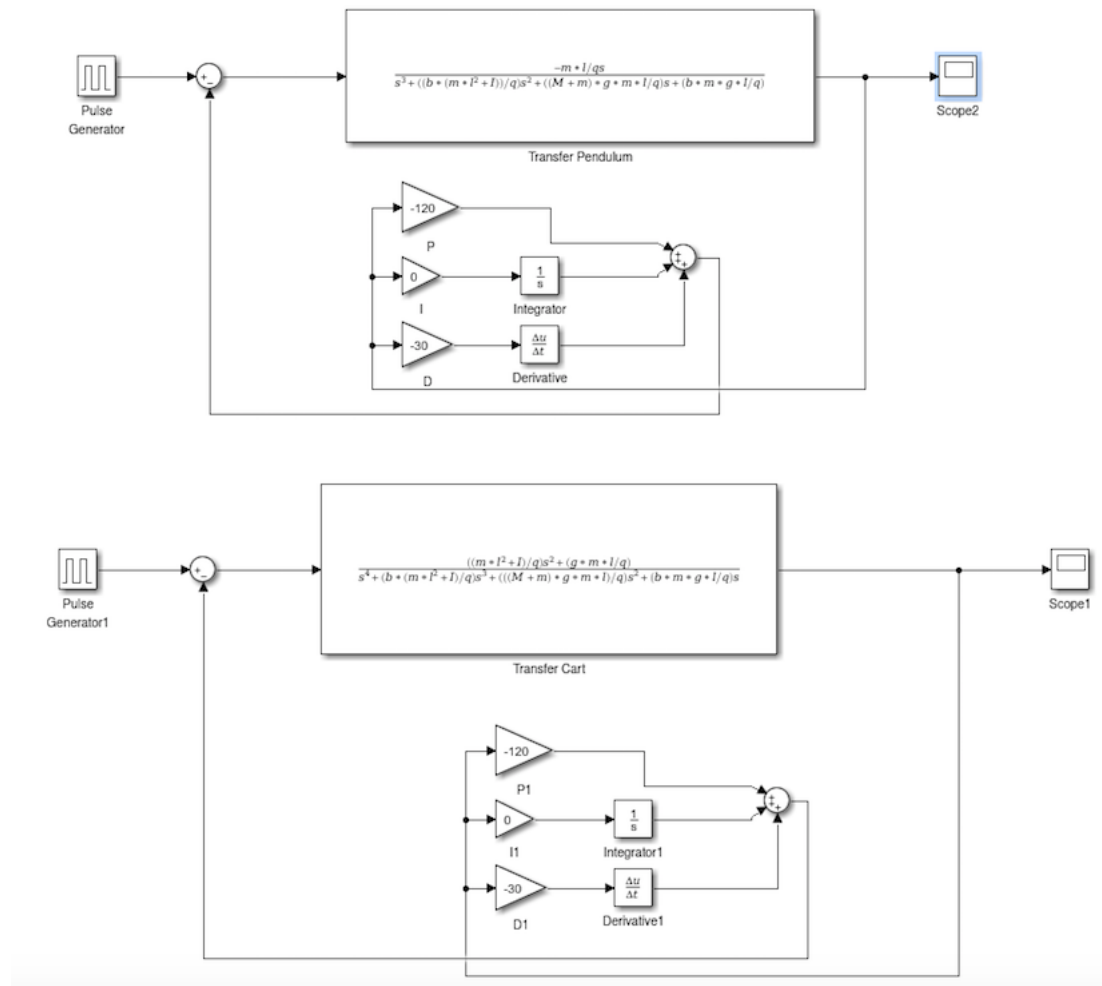


Fig. 71: Simulink model of transfer functions with PID-controller

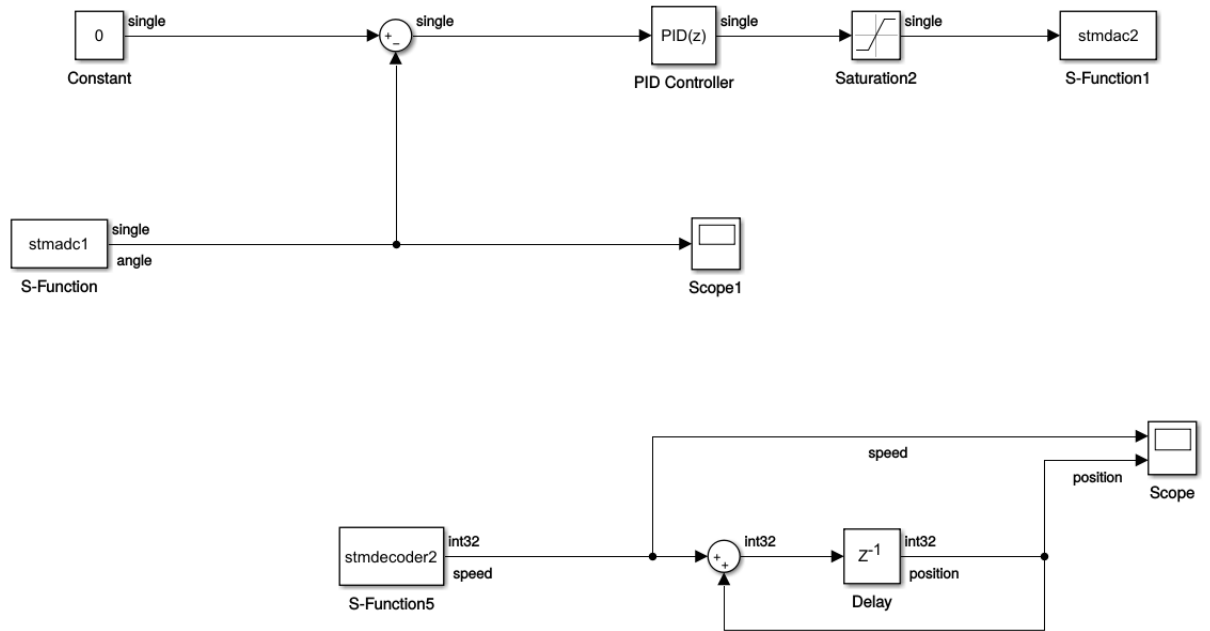


Fig. 72: Simulink model with connection from computer to the position and angle with PID-controller

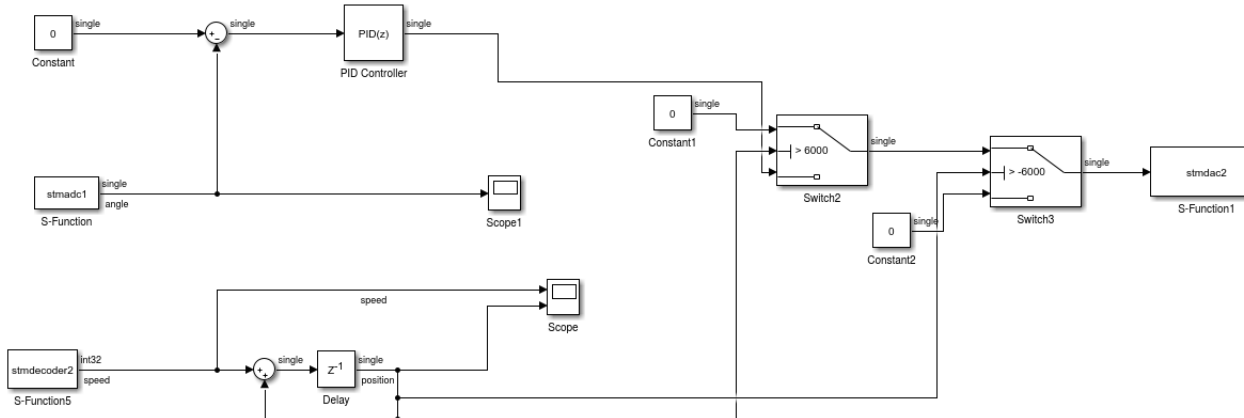


Fig. 73: Simulink model with connection from computer to the position and angle with PID-controller and switch included

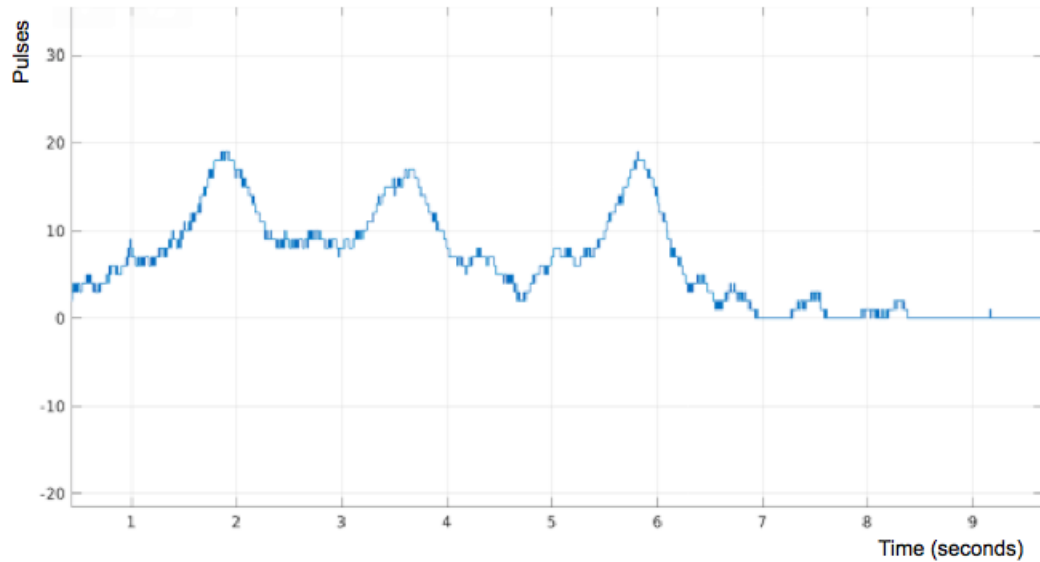


Fig. 74: Scope of the speed of the cart for 10 seconds

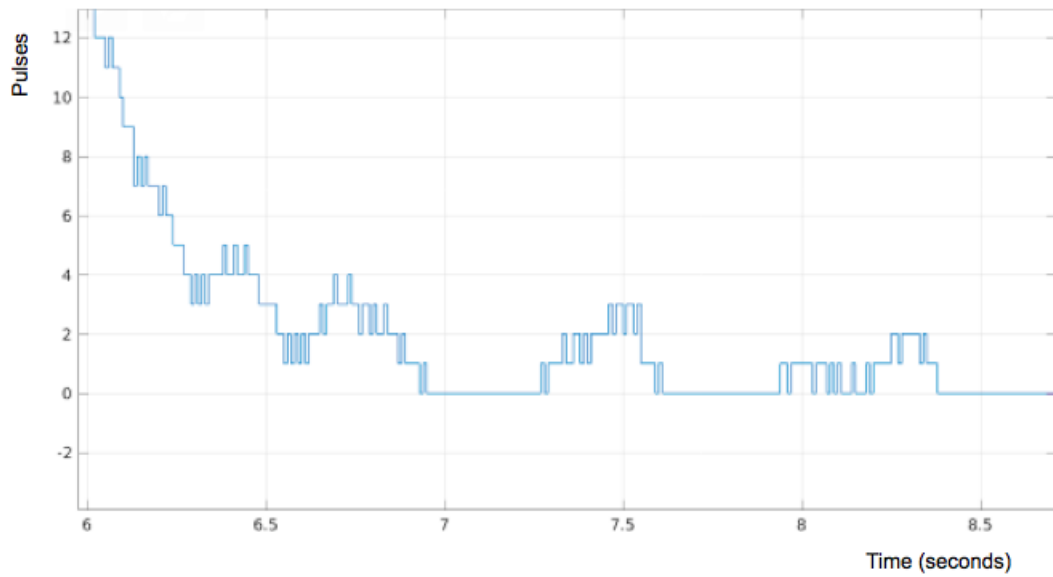


Fig. 75: Scope of the speed of the cart zoomed-in

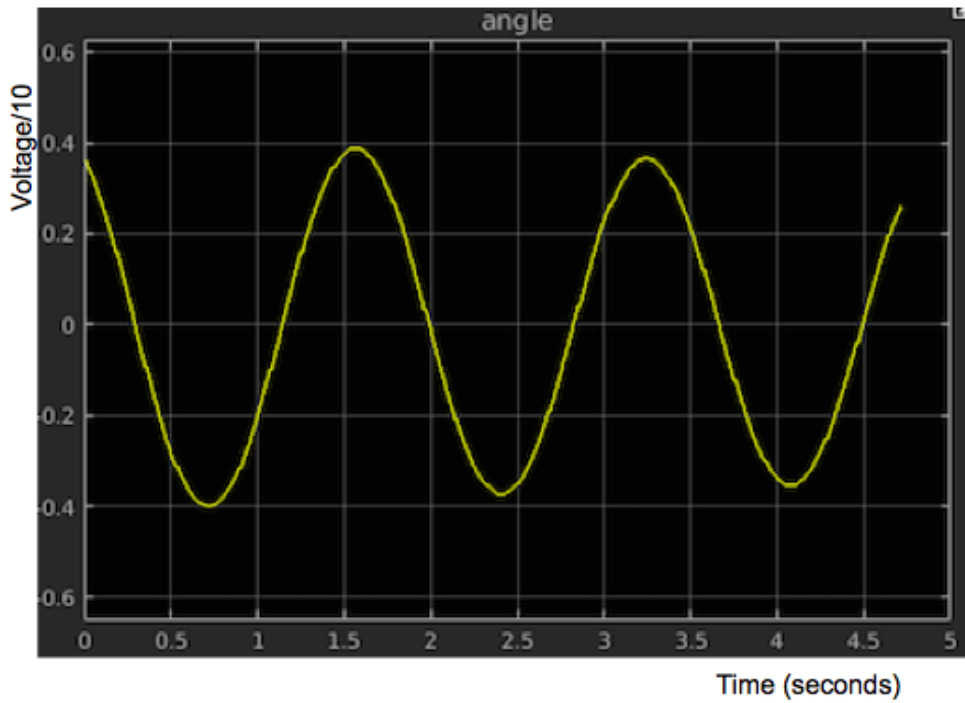


Fig. 76: Scope of the angle from Simulink

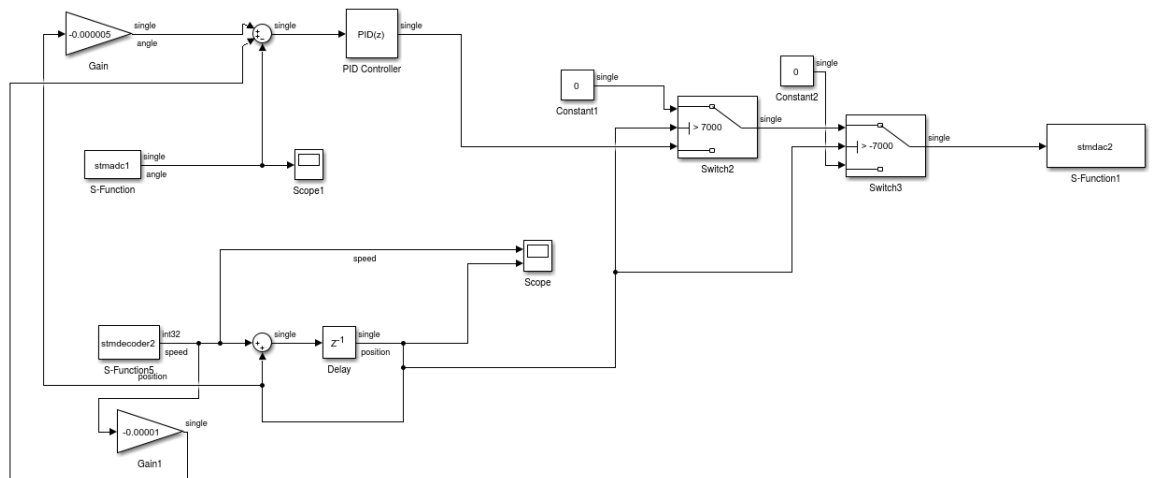


Fig. 77: Final model Simulink

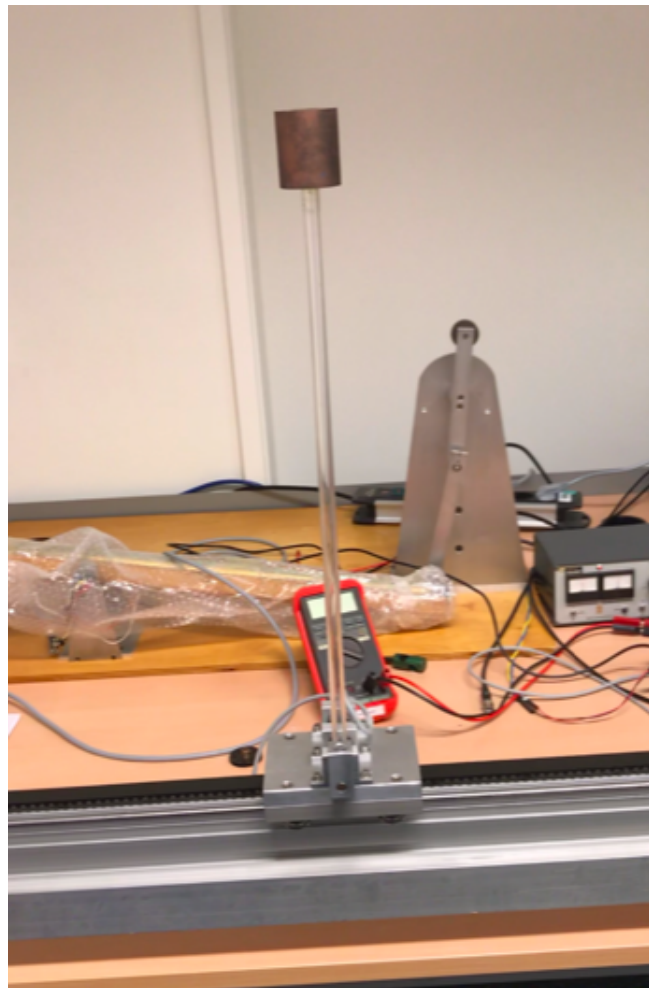


Fig. 78: The hollow, plastic pendulum

## 25 Bibliography

### References

- [1] J.M.A. Scherpen (2018, Feb). Discrete Technology and Production Automation. *Engineering and Technology institute Groningen*,  
<https://www.rug.nl/research/discrete-technology-production-automation/>
- [2] Stuflesser, M., Brandner, M. (2008). Vision-Based Control of an Inverted Pendulum using Cascaded Particle Filters, *Institute of Electrical Measurement and Measurement Signal Processing, Graz University of Technology*,  
[http://www.manuelstuflesser.net/stuflesser\\_paper.pdf](http://www.manuelstuflesser.net/stuflesser_paper.pdf)
- [3] Eco-modules RG, Motive Systems. Eco 30/60, nr. 02251/1/02, *Isotec*
- [4] Encoder Line Drivers, HEDL-550x/554x, HEDL-560x/564x, HEDL-9000/9100, HEDL- 9040/9140/ 92xx, *Avago Technologies*
- [5] Resistor Guide (2018). Potentiometer,  
<http://www.resistorguide.com/potentiometer/>
- [6] Agarwal, T (2015). The Working Principle of a PID controller for beginners. *Elprocus*  
<https://www.elprocus.com/the-working-of-a-pid-controller/>
- [7] Isaksson, A. (1999). Model based control design. Supplied as supplement to course book in Automatic Control Basic course,  
<https://www.kth.se/social/upload/4fce19f8f276544184000008/IMCkomp.pdf>
- [8] Hevner, A. R. (2007). A three cycle view of design science research. *Scandinavian Journal of Information Systems*, 19(2), 88.
- [9] natuurkundemitgelegd.nl (2018). Harmonische trilling, slinger, massaveer. <https://www.kth.se/social/upload/4fce19f8f276544184000008/IMCkomp.pdf>

- [10] Control Tutorials. Inverted Pendulum: System Modelling  
<http://ctms.engin.umich.edu/CTMS/index.php?example=InvertedPendulumsection=SystemModeling>
- [11] WordPress. Aluminium. <http://www.soortelijkgewicht.com/vaste-stoffen/aluminium>
- [12] NationalInstruments (2018). Encoder measurements: how to guide.  
<http://www.ni.com/tutorial/7109/en/>
- [13] Incremental Rotary Encoder. [https://en.wikipedia.org/wiki/Rotary\\_encoder](https://en.wikipedia.org/wiki/Rotary_encoder)
- [14] RPM Measurement Techniques (2016)  
[http://www.opto22.com/documents/1784\\_rpm\\_measurement\\_techniques\\_technical\\_note.pdf](http://www.opto22.com/documents/1784_rpm_measurement_techniques_technical_note.pdf)
- [15] How to Measure Conveyer Belt Speed with Encoders (2018)  
[https://www.dynapar.com/knowledge/applications/measure\\_conveyor\\_speed\\_with\\_encoders/](https://www.dynapar.com/knowledge/applications/measure_conveyor_speed_with_encoders/)
- [16] Course support: Control Engineering. TBV Lugus  
<https://congressus-tbvlugus.s3-eu-west-1.amazonaws.com/files/0e1a2c020831497aba4c3a8ac8b8bfd3.pdf>
- [17] Control Tutorials. Introduction: PID controller design  
<http://ctms.engin.umich.edu/CTMS/index.php?example=Introductionsection=ControlPID>
- [18] Aalborg Universiteit. Inverted Pendulum. Department of energy control  
<http://vbn.aau.dk/files/31925138/Report>
- [19] DC Servo Motors (2018). Theory of DC Servo Motor  
<https://www.electrical4u.com/dc-servo-motors-theory-and-working-principle/>
- [20] Compound Wound DC Motor or DC Compound Motor (2018)  
<https://www.electrical4u.com/compound-wound-dc-motor-or-dc-compound-motor/>
- [21] Mathematical Modeling of DC Machines. Chapter 1
- [22] DC Compound motor (Definitions, Types, Applications, equations)(2018) <https://www.top-ee.com/dc-compound-motor/>
- [23] National Instrument: Innovation, Compound Motors (2016)  
<http://www.ni.com/white-paper/14920/en/>

- [24] Collin, D. (2015). FAQ: What are DC shunt motors and where are they used? <https://www.sharelatex.com/project/5acf3a3951db74054e1cd7ce>
- [25] Magsino, E. (2009). Speed and torque control of a DC shunt motor [https://www.researchgate.net/publication/272164467\\_SPEED\\_AND\\_TORQUE\\_CONTROL\\_OF\\_A\\_DC\\_SHUNT\\_MOTOR](https://www.researchgate.net/publication/272164467_SPEED_AND_TORQUE_CONTROL_OF_A_DC_SHUNT_MOTOR)